

**Particulate organic carbon-<sup>234</sup>Th relationships in particles separated by settling velocity in the northwest Mediterranean Sea**

Jennifer Szlosek<sup>1\*</sup>, J. Kirk Cochran<sup>1</sup>, Juan Carlos Miquel<sup>2</sup>, Pere Masqué<sup>3</sup>, Robert A. Armstrong<sup>1</sup>, Scott W. Fowler<sup>1,2</sup>, Beat Gasser<sup>2</sup>, David J. Hirschberg<sup>1</sup>

<sup>1</sup>Marine Sciences Research Center, Stony Brook University, Stony Brook, NY 11794-5000, USA

<sup>2</sup>Marine Environmental Laboratories, International Atomic Energy Agency, MC98000, Monaco

<sup>3</sup>Institut de Ciència i Tecnologia Ambientals - Departament de Física, Universitat Autònoma de Barcelona, 08193 Bellaterra, Spain

\*Corresponding author contact information: Jennifer Szlosek; Email: jszlosek@ic.sunysb.edu; Tel: (631) 974-7993; FAX: (631) 632-3066

## Abstract

In order to better understand the relationship between the natural radionuclide  $^{234}\text{Th}$  and particulate organic carbon (POC), marine particles were collected in the northwestern Mediterranean Sea (spring/summer, 2003 and 2005) by sediment traps that separated them according to their *in situ* settling velocities. Particles also were collected in time-series sediment traps. Particles settling at rates of  $>100 \text{ m d}^{-1}$  carried 50% and 60% of the POC and  $^{234}\text{Th}$  fluxes, respectively, in both sampling years. The POC flux decreased with depth for all particle settling velocity intervals, with the greatest decrease (factor of  $\sim 2.3$ ) in the slowly settling intervals ( $0.68\text{--}49 \text{ m d}^{-1}$ ) over trap depths of 524–1918 m, likely due to dissolution and decomposition of material. In contrast the flux of  $^{234}\text{Th}$  associated with the slowly settling particles remained constant with depth, while  $^{234}\text{Th}$  fluxes on the rapidly settling particles increased. Taking into account decay of  $^{234}\text{Th}$  on the settling particles, the patterns of  $^{234}\text{Th}$  flux with depth suggest that either both slow and fast settling particles scavenge additional  $^{234}\text{Th}$  during their descent or there is significant exchange between the particle classes. The observed changes in POC and  $^{234}\text{Th}$  flux produce a general decrease in POC/ $^{234}\text{Th}$  of the settling particles with depth. There is no consistent trend in POC/ $^{234}\text{Th}$  with settling velocity, such as might be expected from surface area and volume considerations. Good correlations are observed between  $^{234}\text{Th}$  and POC, lithogenic material and  $\text{CaCO}_3$  for all settling velocity intervals. Pseudo- $K_d$ s calculated for  $^{234}\text{Th}$  in the shallow traps (2005) are ranked as lithogenic material  $\leq$  opal  $<$  calcium carbonate  $<$  organic carbon. Organic carbon contributes  $\sim 33\%$  to the bulk  $K_d$ , and for lithogenic material, opal and  $\text{CaCO}_3$ , the fraction is  $\sim 22\%$  each. Decreases in POC/ $^{234}\text{Th}$  with depth are accompanied by increases in the ratio of  $^{234}\text{Th}$  to

lithogenic material and opal. No change in the relationship between  $^{234}\text{Th}$  and  $\text{CaCO}_3$  was evident with depth. These patterns are consistent with loss of POC through decomposition, opal through dissolution and additional scavenging of  $^{234}\text{Th}$  onto lithogenic material as the particles sink.

**Keywords:** Thorium, Particulate Organic Carbon, C/Th variability, Settling Rate, Sediment Traps, Mediterranean

## 1 1. Introduction

2 Thorium-234, a particle-reactive radionuclide, is a useful tracer of particle export on  
3 short time scales of days to months ( $t_{1/2} = 24.1$  d) (Coale and Bruland, 1985). The  
4 disequilibrium between  $^{234}\text{Th}$  and its parent,  $^{238}\text{U}$ , results from rapid hydrolyzation of the  
5  $^{234}\text{Th}$  atoms and their adsorption to surface sites of particles (Bruland and Coale, 1986).  
6 This scavenging process leads to a deficit of  $^{234}\text{Th}$  relative to its parent  $^{238}\text{U}$ , which can  
7 be used to determine the flux of thorium out of the upper ocean water column by the  
8 following equation:

$$9 \quad P_{Th} = \lambda \int_{z_2}^{z_1} (A_U - A_{Th,tot}) dz \quad (1)$$

10 where  $P_{Th}$  is the overall flux of  $^{234}\text{Th}$  removed from the depths  $z_1$  to  $z_2$  by the flux of  
11 particles. The  $^{234}\text{Th}$  decay constant is  $\lambda$  ( $0.0288$  d $^{-1}$ ),  $A_U$  is the activity of  $^{238}\text{U}$ , and  $A_{Th,tot}$   
12 is the total activity of  $^{234}\text{Th}$  (Buesseler et al., 1992). The export flux of carbon  $P_{POC}$ ,  
13 through depth  $z_2$  can be calculated as (Buesseler et al., 1992):

$$14 \quad P_{POC} = \frac{POC}{^{234}\text{Th}_p} P_{Th} \quad (2)$$

15 where  $POC/^{234}\text{Th}_p$  is the ratio of POC to  $^{234}\text{Th}$  on particles settling through depth  $z_2$ .  
16 Measurements of  $^{234}\text{Th}/^{238}\text{U}$  disequilibrium and the  $POC/^{234}\text{Th}$  ratio of sinking particulate  
17 matter in the upper ocean have been used increasingly in oceanographic field programs to  
18 estimate the downward flux of particulate organic carbon (POC) from the euphotic zone  
19 (see reviews by Cochran and Masqué, 2003 and Buesseler et al., 2006). It is clear that  
20 the  $POC/^{234}\text{Th}$  ratio (hereafter referred as  $C/^{234}\text{Th}$ ) of marine particles can vary  
21 significantly in space and time due to changes in biological productivity, particle export,  
22 particle size distribution, and acid polysaccharide content of sinking particles.

23 Developing a quantitative understanding of the processes controlling the variability in  
24  $C/^{234}\text{Th}$  ratios of marine particles is thus essential for validating the use of  $^{234}\text{Th}$  to  
25 estimate POC fluxes from the surface ocean (Moran et al., 2003; Buesseler et al., 2006).

26 The MedFlux program used indented rotating sphere (IRS) sediment traps to collect  
27 particles separated by their *in situ* settling velocities. The traps were programmed such  
28 that the carousel collected particles separated into 11 settling velocity intervals ranging  
29 from  $\sim 0.7$  to  $>980 \text{ m d}^{-1}$  throughout the trap deployment (Peterson et al., 2005, 2008).  
30 The IRS sediment traps in settling velocity mode (SV) were deployed along with IRS  
31 sediment traps operated in a in time-series mode (TS) in 2003 and 2005 at the French  
32 JGOFS time-series site, DYFAMED (DYnamique des Flux Atmosphérique en  
33 MEDiterrannée).

34 Here we present  $C/^{234}\text{Th}$  data for samples collected by sediment traps operated in  
35 TS and SV sampling modes. Our goal is to assess sources of variability for the  $C/^{234}\text{Th}$  in  
36 different settling velocity intervals. Samples were collected from the bottom of the  
37 euphotic zone during two spring phytoplankton bloom periods in 2003 and 2005,  
38 respectively. In 2005, additional traps were deployed at mid- and deep-water depths to  
39 evaluate the variability in the  $C/^{234}\text{Th}$  ratio with particle settling velocity, chemical  
40 composition, and depth.

## 41 **2. Methods**

### 42 *2.1 Sample collection*

43 MedFlux sampling occurred at the French JGOFS time-series site, DYFAMED ( $43^\circ$   
44  $25'\text{N}$ ,  $7^\circ 52'\text{E}$ ; water depth  $\sim 2300 \text{ m}$ ), located in the Ligurian Sea, northwest  
45 Mediterranean. Further information on the region is included in the Preface of this

46 volume (Lee et al., this volume). Collection techniques included large volume *in situ*  
47 pumps, moored swimmer-exclusion (IRS) sediment traps, and a large floating sediment  
48 trap, or NetTrap, used to collect fresh, sinking particles below the euphotic zone  
49 (Peterson et al., this volume).

### 50 *2.1.1 Sediment traps*

51 Time-series (TS) traps were deployed from 6 March – 6 May 2003 with cups  
52 collecting over 5- to 6-day time intervals and from 4 March – 1 May 2005 with 5-day  
53 time intervals. Particles with settling velocities from 0.68 to >980 m d<sup>-1</sup> were separated  
54 into 11 settling velocity intervals (Table 1); the intervals were slightly different in 2003  
55 and 2005. Carousel rotation times were changed in 2005 to better resolve material flux  
56 shifts in the faster settling velocities. Further details on the operation of the IRS traps in a  
57 settling velocity mode have been given in Peterson et al. (2005). A single mooring was  
58 used in each deployment period such that time-series and duplicate settling velocity (SV)  
59 traps were deployed on the same array. Of the two SV traps (SV1 and SV2) deployed at  
60 313 m in 2005, SV1 was contaminated; consequently only data from SV2 will be  
61 discussed. The duplicate SV traps at both 524 m and 1918 m in 2005 operated  
62 successfully and allowed us to evaluate reproducibility.

63 The intended trap deployment depths were 200 m in 2003 and 2005 as well as 400 m  
64 and 1800 m in 2005. Actual trap depths were 238 m in 2003 and 313 m, 524 m and 1918  
65 m in 2005. Deployment depths were corrected for the mooring wire angle by using  
66 information provided by current meters mounted on each array. Mean current velocities  
67 at the shallow traps were 4.5 cm s<sup>-1</sup> (238 m) and 12 cm s<sup>-1</sup> (313 m) in 2003 and 2005,  
68 respectively (Cochran et al., this volume).

69 TS and SV trap sampling tubes were split for chemical characterization using a  
70 McLane™ WSD splitter. One split was filtered on 0.4 µm Nuclepore filters for  
71 determination of  $^{234}\text{Th}$  and another was filtered onto Whatman GF/F filters for  
72 measurement of POC. Other splits were taken for organic composition (Wakeham et al.,  
73 this volume), ballast minerals (Lee et al., this volume), and mass flux (Armstrong et al.,  
74 this volume).

75 The length of the sediment trap deployments necessitated the use of poisons to  
76 prevent bacterial decomposition of the captured samples. Sampling tubes were poisoned  
77 with mercuric chloride by a small poison diffuser containing 0.5 g NaCl and 14 mg  
78  $\text{HgCl}_2$  as described in Peterson et al., (2005). A recent study by Liu et al. (2006) has  
79 shown that the use of  $\text{HgCl}_2$  as a poison affects the total abundance of organic matter and  
80 the composition of many classes of organic compounds by abiotic oxidation and  
81 dissolution.  $^{234}\text{Th}$  could be desorbed from particles due to the increased ionic strength of  
82 the mercuric chloride brine. However,  $^{210}\text{Po}$  was measured in the overlying water of each  
83 sampling tube in 2003 and none was detected (Stewart et al., 2007a). We conclude on this  
84 basis that there was little release of  $^{234}\text{Th}$  due to the trap poison.

85

## 86 *2.2 Sample analyses*

### 87 *2.2.1 $^{234}\text{Th}$ activity*

88 Non-destructive beta counting was used to measure  $^{234}\text{Th}$  activities of the particulate  
89 fractions. Filter material was mounted for beta counting according to the methods of  
90 Buesseler et al. (1998) and Cochran et al. (2000; this volume). The beta counting  
91 efficiency ( $0.41 \pm \sim 5\%$ ) was determined by evaporating an aliquot of  $^{238}\text{U}$  (with  $^{234}\text{Th}$  in

92 equilibrium) onto filters mounted in the same manner as the samples. Filters were  
93 counted over 2 half-lives of  $^{234}\text{Th}$  ( $t_{1/2} = 24.1$  days). Errors include the  $1\sigma$  counting error  
94 and appropriate calibration errors.

### 95 2.2.2 Decay correction of SV trap $^{234}\text{Th}$ data

96  $^{234}\text{Th}$  activities must be corrected for decay from the time of measurement to that of  
97 collection. For the time-series traps, this correction is straightforward because the  
98 collection interval is small compared with the half-life of  $^{234}\text{Th}$ . In the case of the settling  
99 velocity traps, the material collected for each settling velocity interval may have entered  
100 the trap uniformly throughout the deployment or at anytime during the trap deployment.  
101 For a sediment trap collecting particles over a long time interval relative to the half-life of  
102  $^{234}\text{Th}$ , the standard method of decay correction, assuming a constant flux of  $^{234}\text{Th}$  during  
103 the collection interval, is to calculate the effective time during the deployment to which  
104 the activity must be corrected (Spencer et al. 1978). If  $t_1$  is the start of the deployment  
105 and  $t_2$  is the recovery, the effective “mid-point” of the deployment for decay-correction of  
106  $^{234}\text{Th}$  activities is  $t_1 + \Delta t$ , where:

$$107 \quad \Delta t = -\frac{1}{\lambda} \ln \left[ \frac{1 - e^{-\lambda(t_2 - t_1)}}{\lambda(t_2 - t_1)} \right] \quad (3)$$

108 Sample  $^{234}\text{Th}$  activities are generally measured some time after trap recovery, but can  
109 readily be corrected for decay from measurement to trap recovery ( $t_2$ ). The appropriate  
110 factor (F) by which activities at trap recovery should be multiplied for decay-correction is  
111 then

$$112 \quad F = 1 / e^{-\lambda(T - \Delta t)} \quad (4)$$

113 where  $T = t_2 - t_1$ . This correction was applied erroneously in Spencer et al. (1978) because  
114 they corrected radionuclide activities at the time of trap recovery by a factor of  
115  $1/e^{-\lambda\Delta t}$  rather than the formulation in Eqn. 4

116 For the shallow traps in 2003 and 2005, we have time-series records of the  $^{234}\text{Th}$  flux  
117 that clearly show variation throughout the SV trap deployments (Fig. 1, 2). Thus an  
118 alternate approach is to use the variation in  $^{234}\text{Th}$  flux with time as recorded in the TS  
119 traps to calculate a correction factor (F) that can be applied to the SV trap samples. We  
120 determine F by applying a decay-weighted averaging procedure to the TS trap record:

$$121 \quad F = \frac{\sum_i \frac{dpm_i}{e^{-\lambda\Delta t_i}}}{\sum_i dpm_i} \quad (5)$$

122 where  $dpm_i$  is the activity in TS cup  $i$  at the time of trap recovery,  $\lambda$  is the decay constant  
123 for  $^{234}\text{Th}$  and  $\Delta t_i$  is the time between recovery and the midpoint of TS cup  $i$ . This  
124 procedure assumes that the temporal pattern of  $^{234}\text{Th}$  flux as recorded in the time-series  
125 trap was the same for all the settling velocity fractions. If the  $^{234}\text{Th}$  flux is constant with  
126 time, Eqn. 5 yields results identical to Eqn. 4.

127 The two methods give decay correction factors that agree to within ~10%. The  
128 correction factors assuming constant flux into the SV trap (Eqn. 4) were 2.72 and 2.44 for  
129 2003 and 2005, respectively. The correction factors calculated taking the TS temporal  
130 variation of  $^{234}\text{Th}$  flux into account (Eqn. 5) were 2.91 and 2.73 for 2003 and 2005,  
131 respectively. Time-series traps deployed with the deep SV traps (524 m, 1918 m) in  
132 2005 did not function, and, in correcting the deep trap  $^{234}\text{Th}$  data for decay, we have  
133 assumed that the temporal variation in  $^{234}\text{Th}$  flux observed in the shallow trap applied at  
134 depth as well. In fact,  $^{234}\text{Th}$  data from a TS trap deployed at 924 m in 2005 gave a decay-

135 correction factor (Eqn. 5) of 2.52, in reasonably good agreement with that from the 313 m  
136 trap ( $F = 2.73$ ). In reporting the SV trap  $^{234}\text{Th}$  data (Table 1) for 2003 and 2005, we use  
137 the decay-correction factors derived from Eqn. 5 applied to the shallow TS traps in each  
138 year. If information is lacking on variations in  $^{234}\text{Th}$  flux coincident with the collection  
139 of particles in SV traps, decay-correction factors for  $^{234}\text{Th}$  must be calculated using Eqns.  
140 3 and 4.

141 We checked the validity of using Eqn. 5 for decay correction by comparing the total  
142  $^{234}\text{Th}$  dpm captured in the SV trap to that of the TS traps at the same depths. In 2003 the  
143 time-integrated decay-corrected  $^{234}\text{Th}$  fluxes in the SV traps were  $36.7 \times 10^3 \text{ dpm m}^{-2}$  and  
144  $45.9 \times 10^3 \text{ dpm m}^{-2}$  for SV1 and SV2, respectively (Table 1). For SV1 and SV2 these  
145 were factors of  $\sim 0.7$  and  $\sim 0.8$ , respectively, less than the time-integrated  $^{234}\text{Th}$  flux  
146 measured in the TS trap ( $51.7 \times 10^3 \text{ dpm m}^{-2}$ ). However, the SV traps also accumulated  
147 less total mass of material than did the TS trap, by factors of  $\sim 0.8$  and  $\sim 0.9$  for SV1 and  
148 SV2 respectively. Thus perhaps the differences in the integrated  $^{234}\text{Th}$  activity among the  
149 TS and SV traps may be due, in part, to variability in the fluxes entering duplicate traps at  
150 a single depth. Offsets between the TS and SV traps at 313 m also were evident in 2005;  
151 the integrated  $^{234}\text{Th}$  and mass fluxes in the SV trap were 1.1 and 1.4 times, respectively,  
152 those of the TS trap. We conclude that these differences are principally related to the  
153 ability of traps operated in different modes at the same depth to capture comparable  
154 fluxes and particle types.

### 155 *2.2.3 POC measurements*

156 Prior to POC analyses, inorganic carbon was removed by fuming the samples with  
157 concentrated HCl. Two replicate splits of the trap material collected in each sample tube

158 for both the TS and SV traps were designated for POC and total carbon (TC)  
159 measurements. The trap splits were filtered onto combusted GF/F filters. POC and TC  
160 were measured on all punches using a Carlo Erba model 1602 CNS analyzer. All carbon  
161 measurements were blank-corrected and had an error of  $\pm 5\%$ .

162

### 163 **3. Results**

#### 164 *3.1. $^{234}\text{Th}$ and OC fluxes in shallow time-series traps-2003 and 2005*

165 During the first two weeks of the 2003 trap deployment, the OC flux was nearly 3  
166 times higher than the trap time-weighted average of  $2.3 \text{ mmol m}^{-2} \text{ d}^{-1}$  (Fig. 1A; Table 1).  
167 The maximum OC flux coincided with a period of high sea surface chlorophyll observed  
168 by satellite (see Lee et al., this volume). OC flux then decreased, dropping an order of  
169 magnitude by DOY 90. Mass flux generally followed OC flux patterns, with maximum  
170 values of  $\sim 1000 \text{ mg m}^{-2} \text{ d}^{-1}$  (Lee et al., this volume). Correspondingly,  $^{234}\text{Th}$  flux  
171 followed the temporal trends of OC flux (Fig. 1A).

172 Similar to 2003,  $^{234}\text{Th}$  and OC fluxes in the shallow trap in 2005 were highest at the  
173 beginning of the trap deployment period (Fig. 2A). The time-weighted average OC flux  
174 was  $1.3 \text{ mmol m}^{-2} \text{ d}^{-1}$ . Mass flux peaked at  $\sim 900 \text{ mg m}^{-2} \text{ d}^{-1}$ , and again the pattern in the  
175 OC flux with time mirrored that of mass flux. The range of  $^{234}\text{Th}$  flux values over the 55  
176 day deployment was comparable to that in 2003 (Fig. 2A; Table 1). The average  $^{234}\text{Th}$   
177 flux for the spring 2005 deployment was approximately equivalent to that in 2003 ( $\sim 1200$   
178  $\text{dpm m}^{-2} \text{ d}^{-1}$ ), whereas the average OC flux was a factor of 2 smaller.

179

#### 180 *3.2. $C/^{234}\text{Th}$ ratios in time-series traps*

181  $C/^{234}\text{Th}$  ratios did not vary significantly with time in 2003 (Fig. 1B). Values ranged  
182 from  $1.8 \pm 0.2$  and  $3.6 \pm 0.2$   $\mu\text{mol/dpm}$  with a time-weighted average of  $2.8 \pm 0.1$   
183  $\mu\text{mol/dpm}$  (Table 1). Conversely, the  $C/^{234}\text{Th}$  ratio of the 2005 313 m TS trap  
184 demonstrated a marked change over the trap deployment. During the first half of the  
185 deployment (DOY 65 to 90) there was little variation in the  $C/^{234}\text{Th}$ , averaging  $0.9 \pm 0.01$   
186  $\mu\text{mol/dpm}$ ; however, after DOY 90 the  $C/^{234}\text{Th}$  steadily increased (Fig. 2B). Over the 55  
187 d deployment the  $C/^{234}\text{Th}$  ratios ranged from  $0.8 \pm 0.02$  to  $4.1 \pm 0.4$   $\mu\text{mol/dpm}$  and the  
188 time-weighted average  $C/^{234}\text{Th}$  ratio for the entire deployment was  $1.1 \pm 0.03$   $\mu\text{mol/dpm}$   
189 (Table 1). The mean TS trap  $C/^{234}\text{Th}$  values in 2003 and 2005 were lower than prior trap-  
190 derived  $C/^{234}\text{Th}$  measurements made at the DYFAMED site ( $4.9 \pm 0.2 - 7.8 \pm 0.3$   
191  $\mu\text{mol/dpm}$ ; Schmidt et al., 2002).

### 192 *3.3. Fluxes in Settling Velocity Traps*

193 The SV trap collects material for the settling velocity intervals throughout the  
194 duration of the trap deployment. Calculation of an average flux in each settling velocity  
195 interval is not possible because of uncertainty in the constancy of the flux with time.  
196 Different settling velocity intervals were used in 2005 than in 2003 to increase the  
197 resolution of the faster settling velocity intervals where fluxes were greatest in 2003, but  
198 this made it difficult to compare directly the results from the two years. To facilitate the  
199 analysis of SV trap data from both years and different depths we use a calculated  
200 parameter referred to as the time-integrated flux density (FD; see Armstrong et al., this  
201 volume). Used in the sense of “probability density”, the FD indicates the probability or  
202 frequency that part of the total trap flux fell at a rate a specified settling velocity interval.  
203 We define FD as the time-integrated flux (the amount of a chemical constituent per

204 square meter integrated over the trap deployment period; e. g., mmol C m<sup>-2</sup> or dpm <sup>234</sup>Th  
205 m<sup>-2</sup>) for an individual SV sediment trap sampling tube divided by the settling velocity  
206 interval (SVI<sub>*i*</sub>) for that sampling tube. The unit-less quantity of the settling velocity  
207 interval (SVI<sub>*i*</sub>) is the log of the maximum settling velocity – log of the minimum settling  
208 velocity (SVI<sub>*i*</sub> = log(SV<sub>max,*i*</sub>) - log(SV<sub>min,*i*</sub>)) for each settling velocity interval, *i*. This  
209 normalized flux, FD, allows one to compare how the total flux is distributed over the  
210 spectrum of settling velocities in different years from observing the box heights as seen in  
211 Figs. 3 and 4. Furthermore, one may examine the total trap flux between years by  
212 comparing the summed areas of all boxes, which represent the time-integrated fluxes  
213 over the period of deployment. The OC and <sup>234</sup>Th time-integrated fluxes will henceforth  
214 be referred to as the OC<sub>*i*</sub> and <sup>234</sup>Th<sub>*i*</sub> where *i* designates the settling velocity interval and  
215 the units are the total mmol C m<sup>-2</sup> or total dpm <sup>234</sup>Th m<sup>-2</sup> captured in that settling velocity  
216 interval over the whole trap deployment (Table 1).

217 In 2003 and 2005, ~ 50% of the OC in the shallow traps (238 m and 313 m) settled at  
218 rates ≥ 100 m d<sup>-1</sup> (Figs. 3A and 3D). Similarly, a large portion of the <sup>234</sup>Th settled at rates  
219 > 100 m d<sup>-1</sup> for both years. The >100 m d<sup>-1</sup> portion of the settling velocity spectrum had  
220 57% and 69% of the <sup>234</sup>Th in the 2003 SV1 and SV2 traps, respectively, and 59% of the  
221 <sup>234</sup>Th in the 2005 shallow SV trap (Figs. 3B and 3E). The greatest proportion of OC and  
222 <sup>234</sup>Th fell within the settling velocity range of 196 to 490 m d<sup>-1</sup>. This settling velocity  
223 interval contained nearly 26% (SV1 only) and ~24% of the total OC for 2003 and 2005,  
224 respectively, and 30–40% of the <sup>234</sup>Th (Table 1). In 2003 and 2005, the OC FD loosely  
225 followed the mass FD trends with settling velocity (Lee et al., 2008; Armstrong et al.,  
226 2008).

227

228 *3.4. Variation of  $C/^{234}\text{Th}$  with settling velocity in shallow SV traps-2003 and 2005*

229 The  $C/^{234}\text{Th}$  ratios of the shallow SV traps of 2003 and 2005, did not demonstrate a  
230 discernable trend with settling velocity (Figs. 3C and 3F, respectively, Table 1). The  
231 weighted average  $C/^{234}\text{Th}$  in 2003 was  $3.4 \pm 0.1$  for SV1 (Table 1). Ignoring the  
232 maximum at  $98\text{--}196 \text{ m d}^{-1}$  for 2003 SV1, the  $C/^{234}\text{Th}$  ratios of individual settling velocity  
233 intervals varied less than 30% in 2003 and in 2005. The weighted average  $C/^{234}\text{Th}$  for  
234 2005 ( $1.2 \pm 0.03 \text{ } \mu\text{mol/dpm}$ ) agreed well with the time-weighted average for the TS trap  
235 deployed on the same array ( $1.1 \pm 0.03 \text{ } \mu\text{mol/dpm}$ ) and was a factor of  $\sim 3$  less than the  
236 weighted average values for 2003. In 2005, there was no single settling velocity interval  
237 that demonstrated a clear peak in the  $C/^{234}\text{Th}$  ratio as was seen in 2003 (Figs. 3C, F).  
238 Moreover, the settling velocity intervals covering the range of  $98\text{--}196 \text{ m d}^{-1}$  generally  
239 had lower  $C/^{234}\text{Th}$  ratios in 2005, possibly indicating compositional differences between  
240 the 2003 and 2005 fast settling particles.

241

242 *3.5 Variation of OC,  $^{234}\text{Th}$  and  $C/^{234}\text{Th}$  in SV traps with depth (2005)*

243 In 2005, 60% of the time-integrated OC flux ( $OC_i$ ) occurred in the fast settling  
244 velocity intervals at 313, 524, and 1918 m (Fig. 4A). The probability that material will  
245 settle at intermediate settling velocities drops sharply at velocities lower than  $326\text{--}490 \text{ m}$   
246  $\text{d}^{-1}$  and  $196\text{--}326 \text{ m d}^{-1}$  for the shallowest trap (Table 1). The total OC collected in each  
247 trap decreased with depth (Table 1).

248 As with OC flux density, the  $^{234}\text{Th}$  flux densities were high at settling velocities of  
249  $196\text{--}980 \text{ m d}^{-1}$ , and decreased within the intermediate settling velocity intervals.

250 Conversely, there was a slight increase in the  $^{234}\text{Th}$  FD within the slowest settling  
251 velocity intervals (Fig. 4B). The time-integrated  $^{234}\text{Th}$  flux ( $^{234}\text{Th}_i$ ) at 1918 m was higher  
252 (mean  $104 \times 10^3 \text{ dpm m}^{-2}$ ) than those at 313 m and 524 m (both  $\sim 80 \times 10^3 \text{ dpm m}^{-2}$ ),  
253 largely due to higher  $^{234}\text{Th}$  FDs in the faster settling velocity intervals at 1918 m relative  
254 to the other depths (Table 1). The weighted average  $C/^{234}\text{Th}$  decreased with depth, with  
255 values of  $1.2 \pm 0.03 \text{ } \mu\text{mol/dpm}$ ,  $0.96 \pm 0.02 \text{ } \mu\text{mol/dpm}$ ,  $0.47 \pm 0.01 \text{ } \mu\text{mol/dpm}$  at 313 m,  
256 524 m, and 1918 m, respectively (Table 1; Fig. 4C). Some overlap was evident in a few  
257 SV intervals at 313 m and 524 m, while the  $C/^{234}\text{Th}$  ratios at 1918 m were generally  
258 lower than those at the shallower depths in all size classes (except the most rapidly  
259 settling; Fig. 4C).

## 260 **4. Discussion**

### 261 *4.1 Controls on $C/^{234}\text{Th}$ variation with settling velocity in shallow traps*

262 There is no clear trend of  $C/^{234}\text{Th}$  with settling velocity in the shallow traps in either  
263 2003 or 2005 (Figs. 3C, F). The  $C/^{234}\text{Th}$  ratio might be expected to increase with  
264 increasing settling velocity, if settling velocity increases with particle dimension and if  
265 POC correlates with particle volume while  $^{234}\text{Th}$  correlates with surface area. However,  
266 increases in  $C/^{234}\text{Th}$  with settling velocity are not evident in the data (other than increases  
267 from the  $0.7\text{--}5.4 \text{ m d}^{-1}$  to the  $5.4\text{--}11 \text{ m d}^{-1}$  interval and from the  $490\text{--}980 \text{ m d}^{-1}$  to the  
268  $>980 \text{ m d}^{-1}$  interval, indicated by the arrows in Fig. 4C). Instead, particle composition  
269 and type are the dominant factors in controlling  $C/^{234}\text{Th}$  in the shallow traps. Additional  
270 factors related to changes in C and  $^{234}\text{Th}$  as particles settle through the water column  
271 affect  $C/^{234}\text{Th}$  in the deeper SV traps (see below). Organic compositional data show that  
272 the slowly settling particles in 2003 were bacterially-reworked material, while the rapidly

273 settling material consisted of fecal pellets and fresh and aggregated diatoms (Wakeham et  
274 al., this volume). These basic differences in particle type will affect the  $C/^{234}\text{Th}$  ratio;  
275 fecal pellets will have low ratios (Rodriguez y Baena et al., 2007), while fresh  
276 phytoplankton will tend to have higher ratios. Indeed, Stewart et al. (2007b) noted a  
277 consistent variation in  $C/^{234}\text{Th}$  (as well as  $C/^{210}\text{Po}$ ) with particle type in the 2003 time-  
278 series trap at 238 m, with the ratios varying in the sequence: fresh phytoplankton >  
279 degraded material > fecal pellets. In the time-series trap, these variations are displayed  
280 with time as the bloom progresses. The SV traps sort the particles into settling velocity  
281 intervals throughout the deployment, but to the extent that fresh and degraded material  
282 and fecal pellets have different settling velocities, the trends seen in the TS trap are  
283 preserved in the SV trap as the settling particles are sorted into settling velocity intervals.

284       Organic compositional analyses of material from the 2005 traps are not complete, but  
285 visual observations of the material suggest fewer diatoms and gelatinous zooplankton and  
286 more crustacean zooplankton relative to 2003. These differences are consistent with  
287 lower  $C/^{234}\text{Th}$  ratios in 2005 relative to 2003 (Fig. 3C, F).

288

#### 289 *4.2. Effect of changes in OC with depth on $C/^{234}\text{Th}$ of settling particles*

290       Recent publications reviewing the use of  $^{234}\text{Th}$  as a POC export proxy have  
291 addressed a number of possible sources for  $C/^{234}\text{Th}$  variability (e.g., Cochran and  
292 Masqué, 2003; Moran et al., 2003, Buesseler et al. 2006). These include preferential loss  
293 or uptake of POC, degradation of the particles, decrease in the volume to surface area  
294 (V:SA) of sinking particles, and preferential adsorption of  $^{234}\text{Th}$  by acidic  
295 polysaccharides (Buesseler et al., 1995, 2006; Burd et al., 2000; Quigley et al., 2002;

296 Moran et al., 2003; Passow et al., 2006; Santschi et al., 2006). We are able to consider  
297 some of these possibilities using the 2005 SV data at 313 m, 524 m, and 1918 m. To our  
298 knowledge, these data comprise the first record in the literature of changes with depth in  
299 the chemical composition of particles separated according to settling velocity.

300 The time-integrated flux densities for OC (Fig. 4A) are similar for the shallow traps  
301 (313 m and 524 m) at fast settling velocities (98–980 m d<sup>-1</sup>). Between 313 m and 524 m  
302 there is relatively little change in flux of OC with depth in the rapid settling velocity  
303 intervals (Fig. 4A). This may indicate that when material is settling at fast rates,  
304 significant alteration of material by degradation does not occur over depths of ~200 m.  
305 Between the 524 m and 1918 m traps, there is a 25-36% decrease in  $OC_i$  for the four  
306 settling velocity intervals in the range of 140–980 m d<sup>-1</sup> (Fig. 4A; Table 1). The %OC on  
307 a mass basis decreases by a factor of ~1.6 from 524 m to 1918 m for these settling  
308 velocity intervals. Indeed, the decrease of bulk OC with depth observed in this study has  
309 been documented previously in sediment traps from the DYFAMED site (Miquel et al.,  
310 1994).

311 OC decreases significantly within the four settling velocity intervals of 10.9–21.8 to  
312 49–98 m d<sup>-1</sup> progressively over the three trap depths (313, 524 and 1918 m; Fig. 4A;  
313 Table 1); the average change in  $OC_i$  in these settling velocity intervals from 313 m to 524  
314 m is ~ 3 mmol C m<sup>-2</sup> and from 524 to 1918 m is ~2 mmol C m<sup>-2</sup>. The %OC of the 10.9–  
315 98 m d<sup>-1</sup> settling velocity intervals also decreased with depth by a factor of ~1.5 for both  
316 depth intervals of 313 m to 524 m and 524 m to 1918 m. As stated previously, the limited  
317 number of samples (duplicates at only two depths: 524 m and 1918 m) does not allow  
318 confidence intervals to be placed on the change in time-integrated OC flux with depth.

319 However, it is likely some of the OC decrease was due to dissolution of POC as a  
320 consequence of cell death as material is exported and undergoes disaggregation and re-  
321 aggregation within the water column (Lee et al., this volume). Goutx et al. (2007) also  
322 show significant loss of C from slowly settling particles collected at the DYFAMED site  
323 in 2003.

324 The loss of OC from the settling particles is accompanied by a decrease in the  
325 C/<sup>234</sup>Th ratio with depth (Fig. 4C). Processes of aggregation, disaggregation and  
326 fragmentation, dissolution and degradation of sinking particles can partly explain the  
327 decreases in %OC and C/<sup>234</sup>Th (Fig. 5A). Through the mesopelagic (or “Twilight Zone”)  
328 organic matter may become the limiting factor in the aggregate matrix, maintaining the  
329 role of a glue such that when the aggregate is saturated or reaches its carrying capacity  
330 (Passow, 2004; Hamm, 2003; De La Rocha and Passow, 2006), it is disrupted by the  
331 impinging force of shear erosion resulting from the particle’s fall (Hill, 1998). This  
332 possible mechanism is consistent with our observations from MedFlux as well as the  
333 “ballast hypothesis” (Armstrong et al., 2002; Klaas and Archer, 2002). A more extensive  
334 discussion of the mechanisms controlling the relationship between OC and ballast  
335 minerals is found in this issue in Lee et al. (this volume) and Armstrong et al. (this  
336 volume).

337 Mechanisms for the decrease in OC FD in slowly settling particles with depth  
338 include incorporation into particles settling at faster rates and loss to the DOC and DIC  
339 pools by dissolution or degradation (Fig. 5A). There also may be significant losses of  
340 POC from the fast settling particles between the 524 m and 1918 m traps caused by  
341 disaggregation of the material into smaller particles settling at lower rates. Admittedly,

342 Fig. 5A is an oversimplification of the many biotic and abiotic processes involved in  
343 altering the absolute abundances of OC associated with sinking particles. However,  
344 collection of particles separated by settling velocity is a critical first step in modeling the  
345 rates of processes shown in Fig. 5A.

346

#### 347 *4.3. Effect of changes in $^{234}\text{Th}$ with depth on $C/^{234}\text{Th}$ of settling particles*

348 Unlike the decreases observed in OC FDs of the fast settling material (98–980 m d<sup>-1</sup>)  
349 with depth, the  $^{234}\text{Th}$  FD is highest at 1918 m (Fig. 4B). At the slower settling velocities  
350 (<98 m d<sup>-1</sup>), there is no change in  $^{234}\text{Th}$  flux density with depth, also in contrast to the  
351 pattern in OC (Fig. 4A, B). A simplified conceptual model of the processes affecting  
352  $^{234}\text{Th}$  in settling particles is shown in Fig. 5B. In addition to transformations among  
353 particle settling velocity intervals (mediated by aggregation and disaggregation;  $\beta_1$  and  $\beta_1$   
354 in Fig. 5B) that affect both OC and  $^{234}\text{Th}$ , thorium is also subject to additional scavenging  
355 and decay as particles settle.

356 The topic of  $^{234}\text{Th}$  decay on particles has received recent attention in the context of  
357 its effect on the POC/ $^{234}\text{Th}$  ratios of filterable particles used to calculate the POC export  
358 from the surface (Cai et al., 2006). Cai et al. (2006) observe various trends in POC/ $^{234}\text{Th}$   
359 with size in filterable particles that they attribute to  $^{234}\text{Th}$  decay. Our settling velocity  
360 data allow us to assign times for transit of particles to depth and thus estimate directly the  
361 effect of decay on the  $^{234}\text{Th}$  of the settling particles. Particles in the settling velocity  
362 intervals <49 m d<sup>-1</sup> (0.7–5.44, 5.44–10.9, 10.9–21.8, and 21.8–49 m d<sup>-1</sup>) demonstrate no  
363 change in  $^{234}\text{Th}$  with depth (Fig. 5B) These particles would take 28 to 1991 days to transit  
364 the distance between the 524 m and 1918 m traps and should show significant  $^{234}\text{Th}$

365 decay. The fact that the  $^{234}\text{Th}$  activity is constant with depth suggests that other processes  
366 must add  $^{234}\text{Th}$  to these particle classes as they settle. Such processes include additional  
367 scavenging of  $^{234}\text{Th}$  (via adsorption), the addition of material and associated  $^{234}\text{Th}$  from  
368 the more rapid settling velocity intervals (disaggregation), and the incorporation of high  
369 molecular weight dissolved organic material (>10 kDa) that is rich in acidic  
370 polysaccharides and associated thorium (Quigley et al., 2002, 2006; Passow et al., 2006,  
371 Santschi et al., 2006; Fig. 5A, B). Given the very large effect of decay on these slowly  
372 settling particles, the lack of change in  $^{234}\text{Th}$  activity with depth implies that  
373 disaggregation of large, rapidly settling particles ( $\beta_1$  in Fig. 5B) or additional scavenging  
374 of  $^{234}\text{Th}$  by the slowly settling particles ( $k_1$  in Fig. 5B) are important.

375 In contrast, little change due to decay would be expected for the rapidly settling  
376 particles. Assuming a mean settling rate of  $\sim 600 \text{ m d}^{-1}$  for the fast settling velocities  
377 ( $196\text{--}980 \text{ m d}^{-1}$ ), radioactive decay would cause reductions of less than 10% in the  $^{234}\text{Th}$   
378 activity between 524 m and 1918 m, yet the time-integrated flux density of  $^{234}\text{Th}$  in the  
379 rapidly settling particles increases by a factor of  $\sim 1.3$  between 524 m and 1918 m (Fig.  
380 4B). If the change is due entirely to scavenging of  $^{234}\text{Th}$ , the increase in the integrated  
381 flux of the rapidly settling particles with depth ( $\sim 23 \times 10^3 \text{ dpm m}^{-2}$ ) is equivalent to the  
382 removal of  $\sim 0.01 \text{ dpm }^{234}\text{Th L}^{-1}$  during the trap deployment, if the particles scavenge  
383 continuously over the  $\sim 1400 \text{ m}$  between the traps. This is a small fraction of the total  
384  $^{234}\text{Th}$  present in the deep water at the DYFAMED site ( $\sim 2.7 \text{ dpm L}^{-1}$ ; Cochran et al., this  
385 volume) and the scavenging would not be apparent in water column profiles of  $^{234}\text{Th}$ .

386 Although advective transport of particles carrying  $^{234}\text{Th}$  from long distances into the  
387 vicinity of deep traps is unlikely due to the prevailing currents at the DYFAMED site, it

388 is important also to consider this as a possible mechanism for increasing  $^{234}\text{Th}$  in material  
389 caught in deep traps. The DYFAMED site is generally regarded as being uninfluenced by  
390 coastal waters, and it has been suggested that particle variability is predominantly driven  
391 by local climate effects and phytoplankton growth in the surface waters because a  
392 geostrophic front cuts off coastal inputs (Béthoux et al., 1998; Millot, 1999; Stemmann et  
393 al., 2002). Schröder et al. (2006) showed that infiltration of the deep eastern  
394 Mediterranean water did not occur at the DYFAMED site in 2005. Lateral transport of a  
395 nepheloid layer would provide additional particle surfaces for  $^{234}\text{Th}$  adsorption, but such  
396 a feature is uncommon at the DYFAMED site (Stemmann, 1998).

397       Despite this, the influence of lateral transport on Th profiles and fluxes at the  
398 DYFAMED site may wax and wane depending on variations in the intensity of seasonal  
399 export events (Cochran et al., this issue). Also, a large “statistical funnel” (Siegel et al.,  
400 1990) influences the deep traps, such that the effective lateral transport of particles to  
401 deep traps integrates over a larger area than that of shallow sediment traps due to the  
402 greater amount of time it would take particles to settle to 1918 m (Cochran et al., this  
403 issue).

404       Data from another thorium isotope are needed to fully constrain even the relatively  
405 simple model of coupled Th/particle dynamics shown in Fig. 5B. Cochran et al. (1993,  
406 2000) and Murnane et al. (1996) used  $^{228}\text{Th}$  and  $^{234}\text{Th}$  applied to filterable particles in this  
407 fashion. Indeed, Cai et al. (2006), have proposed that the comparison of the  $^{234}\text{Th}/^{228}\text{Th}$   
408 ratio on large filterable particles collected by *in situ* pump relative to the ratio in the  
409 dissolved phase can be used as to gauge the amount of time for particle aggregation.  
410 Measurements of  $^{228}\text{Th}$  on the 2005 SV and water column samples are in progress. One

411 caveat in incorporating  $^{228}\text{Th}$  into the model of Fig. 5B is that its activity in solution  
412 changes significantly with depth, following its parent  $^{228}\text{Ra}$  (Moore, 1969). Thus to fully  
413 apply the model requires knowledge of  $^{228}\text{Th}$  in the dissolved phase.

414

#### 415 *4.4. Effects of composition on POC and $^{234}\text{Th}$ of trapped material*

416 Additional compound class data will help elucidate the extent of degradation of  
417 organic matter through the water column and its resultant contribution to the decrease in  
418  $\text{C}/^{234}\text{Th}$  with depth. A good correlation between OC and  $^{234}\text{Th}$  in the settling velocity  
419 intervals, coupled with the change in the relationship from the shallow- and mid-water  
420 traps (313, 524 m) to the deep-water trap (1918 m) in 2005 (Fig. 6A) suggest that both  
421 OC and  $^{234}\text{Th}$  are affected by interactions among the settling velocity intervals as the  
422 particles settle (Fig. 5A, B).

423  $^{234}\text{Th}$  is also correlated to varying degrees with the major ballast mineral components  
424 of the flux (lithogenic aluminosilicates, calcium carbonate and opal; Fig. 6B–D). The  
425 correlations with both lithogenic material and  $\text{CaCO}_3$  are good, and there is little change  
426 in the slope of the relationship between  $^{234}\text{Th}$  and  $\text{CaCO}_3$  with depth (Fig. 6C). Indeed,  
427 both total trap  $^{234}\text{Th}$  (dpm) and  $\text{CaCO}_3$  (mg) increase with depth; the percentage of the  
428 contribution of  $\text{CaCO}_3$  to ballast minerals also increases with depth, largely as a result of  
429 the relative loss of opal.

430 In contrast to the correlation between  $^{234}\text{Th}$  and  $\text{CaCO}_3$  (Fig. 6C), the shallow and  
431 deep traps fall into separate groups for the correlation of lithogenic material with  $^{234}\text{Th}$   
432 (Fig. 6B). The total mg of lithogenic material settling into the deep traps is ~90% that  
433 reaching the 524 m traps. This is equivalent to an increase in the specific activity of  $^{234}\text{Th}$

434 with respect to lithogenic material ( $\text{dpm/g}_{\text{lithogenic}}$ ) and suggests that this fraction is  
435 scavenging additional  $^{234}\text{Th}$  with depth. Indeed, the large role played by sinking  
436 lithogenic material in scavenging Th has been emphasized by Luo and Ku (2004). The  
437 correlation of opal with  $^{234}\text{Th}$  is not as good as correlations of lithogenic material or  
438  $\text{CaCO}_3$  with  $^{234}\text{Th}$ , consistent with prior work that showed that opal was not a strong  
439 scavenger of Th (Chase et al., 2002; Luo and Ku, 2004). In addition, the specific activity  
440 of  $^{234}\text{Th}$  with respect to opal ( $\text{dpm/g}_{\text{opal}}$ ) increases with depth, likely due to silica  
441 dissolution (Lee et al., this volume).

442 The slopes of Figures 6A–D can be used to calculate particle-water partition  
443 coefficients ( $K_d$ s) for a pure end-member representing OC or ballast minerals such as  
444 lithogenic material,  $\text{CaCO}_3$  or opal. The particle-water partitioning coefficient or pseudo-  
445  $K_d$  is equal to the specific activity of thorium on the particle ( $\text{dpm } ^{234}\text{Th/g}_i$  where  $i$   
446 represents OC or ballast mineral content) divided by the dissolved  $^{234}\text{Th}$  activity ( $\text{dpm}$   
447  $^{234}\text{Th/g}$  of water) in the water through which the particles sink. Chase et al. (2002) also  
448 referred to sediment trap-derived particle-water partitioning coefficients as ‘pseudo- $K_d$ ’,  
449 but unlike the derivation of Chase et al. (2002), we use measured dissolved  $^{234}\text{Th}$  activity  
450 instead of the total  $^{234}\text{Th}$  activity. We determine the average water column dissolved  
451  $^{234}\text{Th}$  activities using trapezoidal integration of water column  $^{234}\text{Th}$  profiles obtained  
452 during the trap deployment period (Cochran et al., this volume). The dissolved  $^{234}\text{Th}$   
453 activity representative of 0–524 m (2.3 dpm/L) for the shallow traps was derived from  
454 two profiles of water column  $^{234}\text{Th}$  activities (March 9 and 13, 2005) and the dissolved  
455  $^{234}\text{Th}$  activity representing the 0–1918 m (2.4 dpm/L) for the deep traps came from a  
456 single profile that extended to 1800 m (March 13, 2005: Cochran et al., this volume). Via

457 this calculation, we determine a pseudo- $K_d$  using the slopes of the correlation plots (Figs.  
458 6A-D; Table 2).

459 The pseudo- $K_d$ s in the 313 and 524 m traps are ranked in the sequence lithogenic  
460 material  $\leq$  opal  $<$  CaCO<sub>3</sub>  $<$  OC (Table 2). For the 1918 m trap, the ranking is lithogenic  $\leq$   
461 CaCO<sub>3</sub>  $<$  opal  $<$  OC. One must use caution when interpreting pseudo- $K_d$ s from deep trap  
462 data because the slope of the correlation of thorium with organic carbon and ballast  
463 minerals may change as the composition of sinking particles changes due to degradation  
464 and dissolution. For example, the increases in the deep trap pseudo- $K_d$ s for OC and opal  
465 (Table 2) likely result from the decreases in OC and silica from the sinking particles.

466 Our values for the end-member pseudo- $K_d$ s are generally within the range of those  
467 reported elsewhere (Chase et al., 2002; Luo and Ku, 2004; Li, 2005). Luo and Ku (2004)  
468 and Li (2005) used sediment trap data from open ocean sites, including the equatorial  
469 Pacific and the Southern Ocean to determine pseudo-  $K_d$ s for <sup>230</sup>Th and found lithogenic  
470 material to be a strong scavenger of Th, with values on the order of 10<sup>8</sup> g/g. Our results  
471 suggest that the pseudo- $K_d$  for lithogenic material is most similar to opal in the shallow  
472 traps and to CaCO<sub>3</sub> in the deep trap (Table 2). The pseudo- $K_d$  for lithogenic material at  
473 the DYFAMED site is 2 orders-of-magnitude less, and that for opal approximately 10x  
474 greater than the values derived by Chase et al. (2002), Luo and Ku (2004) and Li (2005).  
475 The difference in  $K_d$ s for the lithogenic material at the DYFAMED site relative to the  
476 Equatorial Pacific and Southern Ocean may be due to the fact that pulses of lithogenic  
477 material followed intense dust deposition events in 2005 and are evident in high  
478 percentages of lithogenic material in the fast settling velocity intervals (Lee et al., this  
479 volume). Because this material settled at accelerated rates, <sup>234</sup>Th may not have had time

480 to attain sorption equilibrium before reaching the traps. As well it may have had different  
481 surface area-to-volume characteristics than lithogenic material at open ocean sites.

482 Chase et al. (2002) showed carbonate was at least as important as lithogenic material  
483 for the adsorption of Th and our results this conclusion. Chase et al. (2002) and Luo and  
484 Ku (2004) assumed that the contribution of Th sorption onto organic matter played an  
485 insignificant role in the bulk partition coefficient of Th. We observe the highest Th  
486 pseudo- $K_d$ s for OC in the shallow and deep traps ( $45.4 \times 10^6$  and  $86.3 \times 10^6$ ,  
487 respectively). This may be due to the presence of acidic-rich polysaccharides that form  
488 organic coatings on biogenic particles (Passow, 2002). Indeed, Quigley et al. (2002)  
489 found the  $K_d$  for  $^{234}\text{Th}$  to colloidal organic matter with a high percent of acidic  
490 polysaccharides to be  $\sim 10^8$ . Li (2005) pointed out the importance of including the  
491 contribution of OC to the bulk  $K_d$  of Th and found that it contributed  $22 \pm 6\%$ . Following  
492 the approach of Li (2005), we calculate that OC contributes 33% to the bulk  $K_d$  of  
493 particles settling into the 313 and 524 m traps and 30% to the bulk  $K_d$  in the 1918 m trap  
494 (Table 2).

## 495 **5. Conclusions**

496 The use of sediment traps to collect particles separated by settling velocity permits  
497 relationships among  $^{234}\text{Th}$ , organic carbon and ballast minerals to be determined. Data  
498 from sediment trap deployments in the northwest Mediterranean in spring, 2003 and 2005  
499 show no clear trend in  $C/^{234}\text{Th}$  ratios with settling velocity. Instead variation in  $C/^{234}\text{Th}$   
500 appears to be more strongly influenced by composition of the material, type of particle,  
501 and processes that affect OC and  $^{234}\text{Th}$  with depth such as remineralization and  
502 degradation of OC and the continuous scavenging of  $^{234}\text{Th}$  onto sinking particles.

503 The preponderance of the  $^{234}\text{Th}$  flux is associated with rapidly sinking particles.  
504 Greater than 60% of the  $^{234}\text{Th}$  is associated with particles settling at rates  $>100\text{ m d}^{-1}$ . In  
505 2005, SV traps were deployed at several depths, and the total  $^{234}\text{Th}$  reaching the deep trap  
506 (1918 m) was a factor of 1.3 greater than that reaching the trap at 524 m. The largest  
507 increase in  $^{234}\text{Th}$  was observed for the fast settling velocities (196–980  $\text{m d}^{-1}$ ). The effect  
508 of radioactive decay on  $^{234}\text{Th}$  may be estimated because the settling velocities are known.  
509 Such estimates predict very large decreases in  $^{234}\text{Th}$  for the slowly settling particles and  
510 negligible change for the rapidly settling material. The contrast between predictions and  
511 observations suggests either that  $^{234}\text{Th}$  continues to be scavenged as particles settle, or  
512 there are significant interactions (aggregation, disaggregation) between the fast and  
513 slowly setting particles. In contrast to the pattern seen in  $^{234}\text{Th}$ , organic carbon decreases  
514 by a factor of  $\sim 2$  through the water column, with the greatest decrease in the slowly  
515 settling particles. These changes resulted in a  $\sim 3$ -fold drop in the  $C/^{234}\text{Th}$  ratio with  
516 depth.

517 Correlations between  $^{234}\text{Th}$  and OC,  $\text{CaCO}_3$ , lithogenic material and opal show  
518 varying relationships with trap depth. Good correlations ( $R^2 > 0.8$ ) are evident between  
519  $^{234}\text{Th}$  and OC,  $\text{CaCO}_3$  and lithogenic material. The relationship between  $^{234}\text{Th}$  and  
520  $\text{CaCO}_3$  is similar at all depths, largely because both the total  $^{234}\text{Th}$  (dpm) and the total  
521  $\text{CaCO}_3$  (mg) increase proportionally the same with depth. The ratio of  $^{234}\text{Th}$  to lithogenic  
522 material increases in the 1918 m trap relative to those at 313 m and 524 m, possibly due  
523 to additional scavenging of  $^{234}\text{Th}$  onto this material as it sinks. Decreases in the slope of  
524 the OC- $^{234}\text{Th}$  relationship and the opal- $^{234}\text{Th}$  relationship with depth are due to  
525 decomposition of the organic material and dissolution of opal, respectively. Pseudo- $K_d$ s

526 calculated for the shallow (313 m and 524 m) 2005 traps range from  $5.5 \times 10^6$  for opal to  
527  $45.4 \times 10^6$  for organic carbon. OC provides the greatest contribution to the calculated  
528 bulk Th  $K_d$  (~33%), with lithogenic material,  $\text{CaCO}_3$  and opal each contributing ~22%.  
529 Pseudo- $K_{ds}$  for the deep trap material range from  $5.9 \times 10^6$  for lithogenic material to  $86.3$   
530  $\times 10^6$  for OC, with OC comprising the largest relative contribution (~30%) to the bulk  $K_d$ ,  
531 followed by  $\text{CaCO}_3$ , lithogenic material and opal at 20-26%.

532 Measuring the OC,  $^{234}\text{Th}$ , ballast minerals and organic composition of particles  
533 separated by settling velocity over multiple depths provides valuable information on the  
534 effects of composition and particle dynamics on variations in OC,  $^{234}\text{Th}$  and the  $\text{C}/^{234}\text{Th}$   
535 ratio. With settling velocities and fluxes known, data on additional radionuclides (e.g.  
536  $^{228}\text{Th}$  and  $^{210}\text{Po}$ ) can provide powerful constraints on the rates of transformations and  
537 interactions among settling particles.

### 538 **Acknowledgements**

539 Support for the MedFlux program was provided by the National Science Foundation,  
540 Chemical Oceanography Program and the International Atomic Energy Agency in  
541 Monaco. The IAEA is grateful for the support provided to its Marine Environment  
542 Laboratories by the Government of the Principality of Monaco. We greatly appreciate  
543 Cindy Lee for persistent guidance with the production of this manuscript. We  
544 acknowledge the work of others, namely, M. Peterson, S. Wakeham, L. Abramson, and  
545 Z. Liu, for their sample analyses (including POC and compound class measurements) and  
546 discussion. We thank the reviewers for their comments and suggestions, which were very  
547 helpful and improved this manuscript. This is MedFlux contribution No. 19 and MSRC  
548 contribution No. 1358.

## References

- Armstrong, R.A., Lee, C., Hedges, J. I., Honjo, S., Wakeham, S., 2002. A new, mechanistic model for organic carbon fluxes in the ocean based on the quantitative association of POC with ballast minerals material. *Deep-Sea Research II* 49, 219-236.
- Armstrong, R.A., Lee, C., Peterson, M.L., Cochran, J.K., Wakeham, S.G., 2008. Sinking velocity spectra and the ballast minerals ratio hypothesis. *Deep-Sea Research II*, this volume.
- Béthoux, J. P., Prieur, L., 1983. Hydrologie et circulation en Méditerranée Nord-Occidentale. *Pétroles et Techniques* 299, 25-34.
- Bruland, K.W., Coale, K.H., 1986. Surface Water  $^{234}\text{Th}/^{238}\text{U}$  disequilibria: spatial and temporal variations of scavenging rates within the Pacific Ocean. In: Burton, J.D., Brewer, P.G., Chesselet, R. (Eds.), *Dynamic Processes in the Chemistry of the Upper Ocean*. Plenum Press, pp 159-172.
- Buesseler, K., Ball, L., Andrews, J., Benitez-Nelson, C., Belostock, R., Chai, F., Chao, Y., 1998. Upper ocean export of particulate organic carbon in the Arabian Sea derived from thorium-234. *Deep-Sea Research I* 45, 2461-2487.
- Buesseler, K.O., Cochran, J. K., Bacon, M. P., Livingston, H. D., Casso, S. A., Hirschberg, D., Hartman, M. C., Fler, A. P., 1992. Determination of thorium isotopes in seawater by nondestructive and radiochemical procedures. *Deep-Sea Research I* 39, 1103-1114.
- Buesseler, K.O., Benitez-Nelson, C.R., Moran, S.B., Burd, A., Charette, M., Cochran, J.K., Coppola, L., Fisher, N.S., Fowler, S.W., Gardner, W.D., Guo, L.D.,

- Gustafsson, O., Lamborg, C., Masque, P., Miquel, J.C., Passow, U., Santschi, P.H., Savoye, N., Stewart, G., Trull, T., 2006. An assessment of particulate organic carbon to thorium-234 ratios in the ocean and their impact on the application of  $^{234}\text{Th}$  as a POC flux proxy. *Marine Chemistry* 100, 213-233.
- Burd, A.B., Moran, S.B., Jackson, G.A., 2000. A coupled adsorption-aggregation model of the POC/ $^{234}\text{Th}$  ratio of marine particles. *Deep-Sea Research I* 47, 103-120.
- Cai, P., Dai, M., Chen, W., Tang, T., Zhou, K. On the importance of the decay of  $^{234}\text{Th}$  in determining size-fractionated C/ $^{234}\text{Th}$  ratio on marine particles. 2006. *Geophysical Research Letters* 33, L23602, doi: 10.1029/2006GL027792.
- Chase, Z., Anderson, R.F., Fleisher, M.Q., Kubik, P.W., 2002. The influence of particle composition and particle flux on scavenging of Th, Pa and Be in the ocean. *Earth and Planetary Science Letters* 204, 215-229.
- Coale, K.H., Bruland, K.W., 1985.  $^{234}\text{Th}$ : $^{238}\text{U}$  disequilibria within the Californian current. *Limnology and Oceanography* 30, 22-33.
- Cochran, J.K., Buesseler, K.O., Bacon, M.P., Livingston, H.D., 1993. Thorium isotopes as indicators of particle dynamics in the upper ocean: results from the JGOFS North Atlantic Bloom experiment. *Deep-Sea Research I* 40, 1569-1595.
- Cochran, J.K., Buesseler, K.O., Bacon, M.P., Wang, H.W., Hirschberg, D.J., Ball, L., Andrews, J., Crossin, G., Fler, A., 2000. Short-lived thorium isotopes ( $^{234}\text{Th}$ ,  $^{228}\text{Th}$ ) as indicators of POC export and particle cycling in the Ross Sea, Southern Ocean. *Deep-Sea Research II* 47, 3451-4390.
- Cochran, J.K., Masqué, P., 2003. Short-lived U/Th radionuclides in the ocean: tracers for scavenging rates, export fluxes and particle dynamics. In: Bourdon, B., Henderson,

- G.M., Lundstrom, C.C., Turner, S.P. (Eds.), *Reviews in Mineralogy and Geochemistry*, 52, Uranium-series Geochemistry. Mineralogy Society of America, Washington, D.C., pp 461-492.
- Cochran, J.K., Miquel, J-C., Fowler, S.W., Gasser, B., Hirschberg, D.J., Szlosek, J., Rodriguez y Baena, A.M., Armstrong, R.A., Stewart, G., Masque, P., 2008. Time-series measurements of  $^{234}\text{Th}$  in water column and sediment trap samples from the Northwestern Mediterranean. *Deep-Sea Research II*, this issue.
- De La Rocha, C.L., Passow, U., 2006. Accumulation of mineral ballast on organic aggregates. *Global Biogeochemical Cycles* 20, GB1013, doi: 10.1029/2005GB002579.
- Goutx, M., Wakeham, S.G., Lee, C., Duflos, M., Guigue, C., Liu, Z., Moriceau, B., Sempéré, R., Tedetti, M., Xue, J., 2007. Composition and degradation of marine particles with different settling velocities in the northwest Mediterranean Sea. *Limnology and Oceanography* 52, 1645-1664.
- Hamm, C.E., 2002. Interactive aggregation and sedimentation of diatoms and clay-sized lithogenic material. *Limnology and Oceanography* 47, 1700-1795.
- Hill, P.S., 1998. Controls on Flocculation Size in the Sea. *Oceanography*, 11, 13-18.
- Klaas, C., Archer, D.E., 2002. Association of sinking organic matter with various types of mineral ballast minerals in the deep sea: Implications for the rain ratio. *Global Biogeochemical Cycles* 16, 1116, doi: 10/1029/2001GB001765.
- Lee, C., Wakeham, S.G., 1992. Organic matter in the water column – future research challenges. *Marine Chemistry* 39, 95-118.

- Lee, C., Armstrong, R.A., Cochran, J.K., Engel, A., Fowler, S., Goutx, M., Giselher, G., Masqué, P., Miquel, J.C., Peterson, M., Tamburini, C., Wakeham, S., 2008. MedFlux: Investigations of particles in the Twilight Zone. *Deep-Sea Research II*, this issue.
- Lee, C., Peterson, M.L., Wakeham, S.G., Armstrong, R.A., Cochran, J.K., Miquel, J.C., Fowler, S.W., Hirschberg, D., Beck, A., Xue, J., 2008. Particulate matter fluxes measured using Time-Series and Settling Velocity sediment traps in the northwestern Mediterranean Sea. *Deep-Sea Research II*, this volume.
- Li, Y.-H., 2005. Controversy over the relationship between major components of sediment-trap materials and the bulk distribution coefficients of  $^{230}\text{Th}$ ,  $^{231}\text{Pa}$ , and  $^{10}\text{Be}$ . *Earth and Planetary Science Letters* 233, 1-7.
- Liu, Z., Lee, C., Wakeham, S.G. 2006. Effects of mercuric chloride and protease inhibitors on degradation of particulate organic matter from the diatom *Thalassiosira pseudonana*. *Organic Geochemistry* 37, 1003-1018,
- Luo, S., Ku, T.-L., 2004. On the importance of opal, carbonate, and lithogenic clays in scavenging and fractionating  $^{230}\text{Th}$ ,  $^{231}\text{Pa}$  and  $^{10}\text{Be}$  in the ocean. *Earth and Planetary Science Letters* 220, 201-211.
- Millot, C., 1999. Circulation in the Western Mediterranean Sea. *Journal of Marine Systems* 20, 432-442.
- Miquel, J.C., Fowler, S.W., La Rosa, J., Buat-Menard, P., 1994. Dynamics of the downward flux of particles and carbon in the open northwestern Mediterranean Sea. *Deep-Sea Research I* 41, 243-261.
- Moore, W. S., 1969. Measurement of  $^{228}\text{Ra}$  and  $^{228}\text{Th}$  in seawater. *Journal of Geophysical*

Research 74, 694-704.

Moran, S.B., Weinstein, S.E., Edmonds, H.N., Smith, J.N., Kelly, R.P., Harrison, W.G.,

2003. Does  $^{234}\text{Th}/^{238}\text{U}$  disequilibrium provide an accurate record of the export flux of particulate organic carbon from the upper ocean? *Limnology and Oceanography* 48, 1018-1029.

Murnane, R.J., Cochran, J. K., Buesseler, K.O., Bacon, M. P., 1996. Least-squares estimates of thorium, particle, and nutrient cycling rate constants from the JGOFS North Atlantic Bloom Experiment. *Deep-Sea Research I* 43, 239-258.

Passow, U., 2002. Transparent exopolymer particles (TEP) in aquatic environments. *Progress in Oceanography* 55, 287-333.

Passow, U., 2004. Switching perspectives: Do mineral fluxes determine particulate organic carbon fluxes or vice versa? *Geochemistry, Geophysics, Geosystems* 5, Q04002, doi: 10.1029/2003GC000670.

Passow, U., Dunne, J., Murray, J.W., Balistrieri, L., Alldredge, A.L., 2006. Organic carbon to  $^{234}\text{Th}$  ratios of marine organic matter. *Marine Chemistry*, 100: 323-336.

Peterson, M.L., Hernes, P.J., Thoreson, D.S., Hedges, J.I., Lee, C., Wakeham, S.G., 1993. Field evaluation of a valved sediment trap. *Limnology and Oceanography* 38, 1741-1761.

Peterson, M.L., Wakeham, S.G., Lee, C., Askea, M., Miquel, J.C., 2005. Novel techniques for collection of sinking particles in the ocean and determining their settling rates. *Limnology and Oceanography Methods* 3, 520-532.

Peterson, M.L., Fabres, J., Wakeham, S.G., Lee, C., Miquel, J.C., 2008. Sampling the vertical flux in the upper water column using a large diameter free-drifting

- NetTrap adapted to an Indented Rotating Sphere Settling Velocity trap. Deep-Sea Research II, this volume.
- Quigley, M.S., Santschi, P.H., Hung, C.-C., Guo, L., Honeyman, B.D., 2002. Importance of acid polysaccharides for  $^{234}\text{Th}$  complexation onto marine organic matter. *Limnology and Oceanography* 47, 367-377.
- Rodriguez y Baena, A.M., Fowler, S.W., Miquel, J.C., 2007. POC/Natural radionuclide ratios in zooplankton and their freshly produced fecal pellets from the NW Mediterranean. *Limnology and Oceanography* 52, 966-974.
- Santschi, P.H., Murray, J.W., Baskaran, M., Benitez-Nelson, C.R., Guo, L.D., Hung, C.-C., Lamborg, C., Moran, S.B., Passow, U., Roy-Barman, M. 2006. Thorium speciation in seawater. *Marine Chemistry* 100, 250-268.
- Schmidt, S., Andersen, V., Belviso, S., Marty, J.-C., 2002. Strong seasonality in particle dynamics of north-western Mediterranean surface waters as revealed by  $^{234}\text{Th}/^{238}\text{U}$ . *Deep-Sea Research I* 49, 1507-1518.
- Schröder, K., Gasparini, G.P., Tangherlini, M., Astraldi, M., 2006. Deep and intermediate water in the western Mediterranean under the influence of the Eastern Mediterranean Transient. *Geophysical Research Letters* 33, L21607, doi: 10.1029/2006GL07121.
- Siegel, D.A., Deuser, W.G., 1997. Trajectories of sinking particles in the Sargasso Sea: Modeling of statistical funnels above deep-ocean sediment traps. *Deep-Sea Research* 44, 1519-1541.
- Spencer, D. W., Brewer, P. G., Fler, A., Honjo, S., Krishnaswami, S., Nozaki, Y. 1978. Chemical fluxes from a sediment trap experiment in the deep Sargasso Sea.

Journal of Marine Research 36, 493-523.

- Stemmann, L., 1998. Particulate matter spatio-temporal analysis using a new video system, in the north-western Mediterranean Sea. Influence of biological production, terrigenous inputs and hydro-dynamical forcings. Ph.D. Thesis, Universite d'Océanologie Biologie, Paris, France, unpublished.
- Stemmann, L., Gorsky, G., Marty, J.-C., Picheral, M., Miquel, J.C., 2002. Four-year study of large-particle vertical distribution (0–1000 m) in the NW Mediterranean in relation to hydrology, phytoplankton, and vertical flux. *Deep-Sea Research* 9, 2143–2162.
- Stewart, G., Cochran, J.K., Xue, J., Lee, C., Wakeham, S.G., Armstrong, R.A., Masqué, P., Miquel, J.C, 2007a. Exploring the connection between  $^{210}\text{Po}$  and organic matter in the northwestern Mediterranean. *Deep-Sea Research I* 54, 415-427.
- Stewart, G., Cochran, J.K., Miquel, J.C., Masqué, P., Szlosek, J., Rodriguez y Baena, A.M., Fowler, S.W., Gasser, B., Hirschberg, D.J., 2007b. Comparing POC export from  $^{234}\text{Th}/^{238}\text{U}$  and  $^{210}\text{Po}/^{210}\text{Pb}$  disequilibria with estimates from sediment traps in the northwest Mediterranean. *Deep-Sea Research I* 54, 1549-1570.
- Wakeham, S.G., Lee, C., Peterson, M.L., Liu, Z., Szlosek, J., Putnam, I., Xue, J., 2008. Organic compound composition and fluxes in the Twilight Zone - time-series and settling velocity sediment traps during MEDFLUX. *Deep-Sea Research II*, this volume.

## Figure Captions

Fig. 1. 2003 time-series sediment trap data (238 m) A)  $^{234}\text{Th}$  and OC fluxes and B)

$\text{C}/^{234}\text{Th}$  ratio ( $\mu\text{mol C/dpm Th}$ ) ratios.

Fig. 2. 2005 time-series sediment trap data (313 m). A)  $^{234}\text{Th}$  and OC fluxes and B)

$\text{C}/^{234}\text{Th}$  ratio ( $\mu\text{mol C/dpm Th}$ ) ratios.

Fig. 3. A), B), D) and E) histograms of flux density (FD – see text) for 2003 (238 m) and 2005 (313 m) in which the area of the rectangles represent the time-integrated fluxes (OC:  $\text{mmol m}^{-2}$ ;  $^{234}\text{Th}$ :  $\text{dpm m}^{-2}$ ) and the heights of the box and mid-point plotted represent the time-integrated flux densities of OC and  $^{234}\text{Th}$  (OC:  $\text{mmol m}^{-2} \text{SVI}^{-1}$ ;  $^{234}\text{Th}$ :  $\text{dpm m}^{-2} \text{SVI}^{-1}$ ). C) and F)  $\text{C}/^{234}\text{Th}$  ratio values for SV traps. See text and Armstrong et al. (this volume) for explanation of the calculation of time-integrated flux densities.

Fig. 4. Settling velocity plots of OC,  $^{234}\text{Th}$  time-integrated flux densities and  $\text{C}/^{234}\text{Th}$  ratios for 2005: 313 m SV2, average of SV1 and SV2 at 524 m, and the average of SV1 and SV2 at 1918 m. A) Time-integrated flux densities (FD) OC with depth B) Time-integrated FD of  $^{234}\text{Th}$  with depth, and C) the  $\text{C}/^{234}\text{Th}$  ratio with depth. Error bars represent the standard deviation of the duplicate traps. Arrows represent settling velocity intervals where there is an increase in  $\text{C}/^{234}\text{Th}$  with settling velocity.

Fig. 5A. Schematic diagram of the transfers among DOC, POC and DIC pools. Biotic and abiotic losses of POC are represented in a simplified way by dissolution and degradation of POC. The settling of material from one depth horizon to another results in a loss of POC from each settling velocity grouping and is represented by  $S_{slow}$  and  $S_{fast}$ . Exchange between the slow to fast settling pools is indicated by the rate constant  $\beta_1$  representing processes such as aggregation and incorporation POC. Transfer in the opposite direction from fast to slow settling particles might include processes of disaggregation and degradation and is represented by the rate constant  $\beta_{-1}$ .

5B. Schematic diagram of the exchange of  $^{234}\text{Th}$  between dissolved and particulate pools.  $^{234}\text{Th}$  activities of the dissolved ( $A_{diss}$ ), slow settling particles ( $A_{slow}$ ), and fast settling particles ( $A_{fast}$ ) are represented by boxes. The activity of the dissolved parent,  $^{238}\text{U}$ , is denoted by  $A_U$  and the radioactive decay from each phase is represented by  $\lambda$ .  $S_{slow}$  and  $S_{fast}$  represent the loss of particulate thorium by vertical settling. The first-order rate constants of adsorption of dissolved  $^{234}\text{Th}$  onto slow and fast settling particles are  $k_1$  and  $k_2$ , respectively. First-order rate constants for desorption from the slow and fast settling pools are  $k_{-1}$  and  $k_{-2}$ , respectively. Particle exchange is indicated by rate constants  $\beta_1$  for transfer of  $^{234}\text{Th}$  from slow to fast settling particles and  $\beta_{-1}$  for transfer from fast to slow settling particles.

Fig. 6. Correlations of  $^{234}\text{Th}$  with particulate organic carbon and ballast minerals components for shallow SV traps (313 m and 524 m) and deep SV traps (1918 m) of 2005. A) OC vs.  $^{234}\text{Th}$ ; B) Lithogenic particles vs.  $^{234}\text{Th}$ ; C)  $\text{CaCO}_3$  vs.  $^{234}\text{Th}$ , D) opal

as  $\text{SiO}_2 \cdot \text{H}_2\text{O}$  vs.  $^{234}\text{Th}$ . Error bars represent one standard deviation. Best-fit lines for the shallow (313 m and 524 m, solid line) and deep (1918 m, dashed line) trap data are shown with their correlation coefficients,  $R^2$ .

### **Tables**

Table 1. Fluxes and compositional data for Settling Velocity and Time Series Sediment Traps (2003 and 2005)

Table 2. Pseudo- $K_d$ s and trap component weight %s for OC and ballast minerals in 2005 SV sediment trap material

Table 1. Fluxes and compositional data for Settling Velocity and Time Series Sediment Traps (2003 and 2005)

Year	Date	Depth (m)	Trap ID	Settling Velocity		Mass (g m <sup>-2</sup> )	OC <sub>i</sub> (mmol m <sup>-2</sup> )	% OC	<sup>234</sup> Th <sub>i</sub> (10 <sup>3</sup> dpm m <sup>-2</sup> )	C/ <sup>234</sup> Th <sup>†</sup> (μmol dpm <sup>-1</sup> )
				class, <i>i</i> (m d <sup>-1</sup> )	Midpoint date					
2003	6 March-6 May	238	SV1	0.68-1.4	NA	1.32	14.8	12.9	3.37 ± 0.21	4.41 ± 0.29
				1.4-2.7	"	1.37	10.7	9.5	2.90 ± 0.18	3.67 ± 0.23
	2.7-5.4			"	1.19	11.8	12.0	2.71 ± 0.18	4.36 ± 0.30	
	5.4-11			"	0.93	7.4	9.5	1.66 ± 0.16	4.48 ± 0.45	
	11-22			"	0.66	5.6	10.1	1.45 ± 0.15	3.86 ± 0.40	
	22-49			"	0.98	7.2	8.8	1.68 ± 0.09	4.28 ± 0.24	
	49-98			"	1.05	6.2	7.1	1.92 ± 0.16	3.21 ± 0.28	
	98-196			"	1.43	12.3	10.3	1.97 ± 0.16	6.24 ± 0.51	
	196-490			"	5.59	32.1	6.9	13.7 ± 0.94	2.35 ± 0.17	
	490-980			"	1.71	12.7	8.9	4.07 ± 0.25	3.13 ± 0.20	
	>980			"	1.07	2.9	3.2	1.33 ± 0.16	2.15 ± 0.26	
	<b>Total</b>				<b>17.30</b>	<b>123.7</b>	<b>8.5</b>	<b>36.7 ± 1.1</b>	NA	
	<b>Weighted Avg</b>								<b>3.37 ± 0.12</b>	
	2003			238	SV2	0.68-1.4	NA	1.04	10.7	12.3
1.4-2.7		"	0.92			M	M	1.89 ± 0.22	M	
2.7-5.4		"	0.63			4.3	8.2	1.42 ± 0.18	3.03 ± 0.39	
5.4-11		"	0.72			4.3	7.2	2.13 ± 0.19	2.02 ± 0.19	
11-22		"	0.68			5.2	9.2	1.64 ± 0.18	3.19 ± 0.35	
22-49		"	0.77			4.9	7.6	1.94 ± 0.19	2.51 ± 0.25	
49-98		"	1.35			M	M	2.47 ± 0.22	M	
98-196		"	2.68			16.4	7.4	5.35 ± 0.80	3.07 ± 0.46	
196-490		"	8.24			40.5	5.9	18.7 ± 1.47	2.17 ± 0.18	
490-980		"	1.92			13.3	8.3	7.56 ± 0.36	1.76 ± 0.09	
>980		"	0.07			M	M	BD	M	
<b>Total</b>			<b>19.02</b>			<b>99.58</b>	-	<b>45.9 ± 1.8</b>		
<b>Weighted Avg</b>									<b>2.76 ± 0.10</b>	
2003		238	TS			NA	3/8/03	4.03	20.9	6.2
	"			3/13/03	4.13	29.6	8.6	8.58 ± 0.78	3.46 ± 0.32	
	"			3/18/03	4.55	22.1	5.8	11.40 ± 0.73	1.94 ± 0.13	
	"			3/23/03	2.47	18.8	9.2	5.77 ± 0.52	3.27 ± 0.30	
	"			3/28/03	1.06	5.0	5.7	2.98 ± 0.33	1.68 ± 0.19	
	"			4/3/03	0.83	5.7	8.3	1.81 ± 0.14	3.18 ± 0.30	
	"			4/9/03	0.72	6.0	10.0	1.90 ± 0.13	3.15 ± 0.26	
	"			4/15/03	0.94	10.6	13.6	2.92 ± 0.12	3.64 ± 0.20	
	"			4/21/03	0.96	9.8	12.3	3.10 ± 0.11	3.17 ± 0.15	
	"			4/27/03	0.49	6.4	15.7	1.84 ± 0.08	3.50 ± 0.19	
	"			5/3/03	0.92	7.7	10.1	3.01 ± 0.09	2.57 ± 0.10	
	<b>Total</b>				<b>21.09</b>	<b>142.79</b>	<b>8.1</b>	<b>51.7 ± 1.6</b>	NA	
	<b>Weighted Avg</b>								<b>2.76 ± 0.10</b>	
	2005			4 March- 28 April	313	SV2	0.68-5.4	NA	4.88	15.8
5.4-11		"	1.15				5.3	5.5	3.34 ± 0.36	1.59 ± 0.18
11-22		"	1.20				7.5	7.5	3.38 ± 0.34	2.22 ± 0.23
22-49		"	1.28				5.6	5.3	3.94 ± 0.35	1.42 ± 0.13
49-98		"	1.47				8.6	7.0	5.24 ± 0.37	1.64 ± 0.12
98-140		"	1.64				5.8	4.3	4.60 ± 0.38	1.26 ± 0.11
140-196		"	2.16				6.7	3.7	5.55 ± 0.43	1.21 ± 0.10
196-326		"	4.43				12.9	3.5	12.4 ± 0.61	1.04 ± 0.05
326-490		"	4.15				10.2	2.9	11.0 ± 0.54	0.93 ± 0.05
490-980		"	3.42				14.2	5.0	10.7 ± 0.50	1.32 ± 0.07
>980		"	0.33				3.0	11.0	1.64 ± 0.19	1.82 ± 0.22
<b>Total</b>			<b>26.10</b>				<b>95.5</b>	<b>4.4</b>	<b>77.2 ± 1.4</b>	NA
<b>Weighted Avg</b>										<b>1.24 ± 0.03</b>

Continued

Table 1. Fluxes and compositional data for Settling Velocity and Time Series Sediment Traps (2003 and 2005)

Year	Date	Depth (m)	Trap ID	Settling Velocity	Midpoint date	Mass (g m <sup>-2</sup> )	OC <sub>i</sub> (mmol m <sup>-2</sup> )	% OC	<sup>234</sup> Th <sub>i</sub>		C/ <sup>234</sup> Th†	
				class, <i>i</i> (m d <sup>-1</sup> )					(10 <sup>3</sup> dpm m <sup>-2</sup> )	(μmol dpm <sup>-1</sup> )		
		313	TS	NA	3/6/05	4.53	10.9	2.9	12.5	± 0.39	0.87	± 0.03
				"	3/11/05	4.34	10.9	3.0	11.3	± 0.32	0.97	± 0.03
				"	3/16/05	1.64	3.9	2.8	4.4	± 0.21	0.88	± 0.05
				"	3/21/05	2.10	7.2	4.1	7.4	± 0.23	0.96	± 0.04
				"	3/26/05	2.08	6.2	3.6	6.6	± 0.20	0.94	± 0.03
				"	3/31/05	4.40	10.3	2.8	12.5	± 0.23	0.82	± 0.02
				"	4/5/05	1.73	6.8	4.7	4.5	± 0.13	1.52	± 0.05
				"	4/10/05	0.41	2.7	7.8	1.2	± 0.06	2.25	± 0.13
				"	4/15/05	1.35	7.6	6.7	2.3	± 0.08	3.23	± 0.13
				"	4/20/05	0.73	5.7	9.3	1.5	± 0.06	3.85	± 0.17
				"	4/25/05	0.13	1.5	13.4	0.4	± 0.03	4.06	± 0.36
					<b>Total</b>	<b>23.45</b>	<b>73.5</b>	<b>3.8</b>	<b>64.6</b>	<b>± 0.7</b>	NA	
					<b>Weighted Avg</b>						<b>1.14</b>	<b>± 0.03</b>
		524	SV1	0.68-5.4	NA	4.88	13.9	3.4	16.3	± 0.38	0.92	± 0.04
				5.4-11	"	1.23	4.7	4.6	4.50	± 0.20	0.88	± 0.02
				11-22	"	0.93	4.2	5.4	2.94	± 0.15	1.09	± 0.03
				22-49	"	0.88	4.2	5.7	3.04	± 0.15	0.93	± 0.03
				49-98	"	1.01	3.9	4.6	3.46	± 0.15	1.18	± 0.05
				98-140	"	0.98	3.6	4.5	3.13	± 0.15	1.16	± 0.06
				140-196	"	1.23	4.4	4.3	3.72	± 0.15	1.12	± 0.05
				196-326	"	3.04	8.5	3.4	9.17	± 0.23	1.38	± 0.07
				326-490	"	2.84	9.7	4.1	8.89	± 0.22	1.41	± 0.08
				490-980	"	7.00	15.6	2.7	17.8	± 0.29	1.04	± 0.05
				>980	"	1.86	4.6	3.0	4.96	± 0.16	0.85	± 0.03
				<b>Total</b>	"	<b>25.88</b>	<b>77.2</b>	<b>3.6</b>	<b>78.0</b>	<b>± 0.72</b>	NA	
				<b>Weighted Avg</b>							<b>0.99</b>	<b>± 0.02</b>
			SV2	0.68-5.4	NA	5.13	14.1	3.3	16.6	± 0.33	1.48	± 0.10
				5.4-11	"	0.62	4.0	7.7	2.22	± 0.11	1.02	± 0.03
				11-22	"	1.06	3.2	3.6	3.73	± 0.16	0.83	± 0.03
				22-49	"	1.30	4.2	3.9	5.23	± 0.18	0.84	± 0.03
				49-98	"	1.89	5.1	3.2	6.90	± 0.21	1.11	± 0.05
				98-140	"	1.76	5.1	3.5	5.15	± 0.24	1.00	± 0.05
				140-196	"	2.66	7.1	3.2	6.44	± 0.24	0.73	± 0.03
				196-326	"	4.29	9.4	2.6	11.2	± 0.31	0.80	± 0.03
				326-490	"	3.94	9.2	2.8	11.1	± 0.30	0.85	± 0.04
				490-980	"	5.50	14.4	3.1	14.1	± 0.36	1.79	± 0.09
				>980	"	0.75	4.1	6.6	2.78	± 0.17	0.85	± 0.02
				<b>Total</b>	"	<b>28.89</b>	<b>79.8</b>	<b>3.3</b>	<b>85.5</b>	<b>± 0.82</b>	NA	
				<b>Weighted Avg</b>							<b>0.93</b>	<b>± 0.02</b>
		924 m	TS	NA	3/6/05	2.02	6.73	4.0	8.5	± 0.30	0.79	± 0.03
				"	3/11/05	1.93	4.82	3.0	6.2	± 0.24	0.77	± 0.03
				"	3/16/05	2.14	5.02	2.8	8.4	± 0.22	0.60	± 0.02
				"	3/21/05	1.89	5.03	3.2	8.1	± 0.21	0.62	± 0.02
				"	3/26/05	2.56	6.38	3.0	9.9	± 0.20	0.65	± 0.02
				"	3/31/05	3.10	3.28	1.3	10.2	± 0.20	0.32	± 0.01
				"	4/5/05	2.53	5.61	2.7	7.9	± 0.17	0.71	± 0.02
				"	4/10/05	0.47	3.34	8.5	2.2	± 0.09	1.54	± 0.07
				"	4/15/05	0.37	2.63	8.6	1.9	± 0.08	1.42	± 0.07
				"	4/20/05	0.20	2.16	13.3	2.5	± 0.13	0.88	± 0.05
				"	4/25/05	0.47	3.19	8.2	1.6	± 0.06	1.95	± 0.08
					<b>Total</b>	<b>17.67</b>	<b>48.2</b>	<b>3.3</b>	<b>67.2</b>	<b>± 0.62</b>	NA	
				<b>Weighted Avg</b>							<b>0.72</b>	<b>± 0.02</b>

Continued

Table 1. Fluxes and compositional data for Settling Velocity and Time Series Sediment Traps (2003 and 2005)

Year	Date	Depth (m)	Trap ID	Settling Velocity	Midpoint date	Mass (g m <sup>-2</sup> )	OC <sub>i</sub> (mmol m <sup>-2</sup> )	% OC	<sup>234</sup> Th <sub>i</sub>		C/ <sup>234</sup> Th†	
				class, <i>i</i> (m d <sup>-1</sup> )					(10 <sup>3</sup> dpm m <sup>-2</sup> )	(10 <sup>3</sup> dpm m <sup>-2</sup> )	(μmol dpm <sup>-1</sup> )	
		1918	SV1	0.68-5.4	NA	2.73	5.0	2.2	11.5	± 0.26	1.13	± 0.06
				5.4-11	"	0.66	2.0	3.7	2.64	± 0.13	0.46	± 0.01
				11-22	"	0.52	1.5	3.5	2.27	± 0.12	0.43	± 0.01
				22-49	"	0.65	1.6	3.0	3.16	± 0.13	0.40	± 0.01
				49-98	"	0.99	2.4	2.9	4.78	± 0.15	0.49	± 0.02
				98-140	"	1.18	3.9	4.0	5.65	± 0.17	0.69	± 0.03
				140-196	"	1.76	4.0	2.7	8.18	± 0.21	0.50	± 0.02
				196-326	"	3.48	6.1	2.1	15.4	± 0.30	0.51	± 0.02
				326-490	"	4.79	8.4	2.1	19.8	± 0.34	0.66	± 0.04
				490-980	"	6.31	11.3	2.2	24.7	± 0.37	0.75	± 0.04
				>980	"	1.01	4.0	4.7	3.50	± 0.16	0.44	± 0.01
				<b>Total</b>		<b>24.09</b>	<b>50.3</b>	<b>2.5</b>	<b>101.6</b>	<b>± 0.76</b>	NA	
				<b>Weighted Avg</b>							<b>0.50</b>	<b>± 0.01</b>
			SV2	0.68-5.4	NA	3.09	6.9	2.7	17.2	± 0.32	1.38	± 0.15
				5.4-11	"	1.05	3.1	3.6	5.59	± 0.19	0.45	± 0.01
				11-22	"	0.59	1.8	3.6	3.12	± 0.14	0.45	± 0.01
				22-49	"	0.79	2.3	3.5	3.71	± 0.16	0.40	± 0.01
				49-98	"	1.32	3.9	3.5	6.99	± 0.19	0.35	± 0.01
				98-140	"	1.93	2.7	1.7	9.08	± 0.21	0.30	± 0.01
				140-196	"	2.50	4.1	2.0	11.8	± 0.25	0.56	± 0.02
				196-326	"	4.47	7.3	1.9	18.1	± 0.29	0.61	± 0.03
				326-490	"	3.43	5.6	2.0	12.3	± 0.27	0.58	± 0.03
				490-980	"	4.80	7.8	2.0	17.4	± 0.32	0.56	± 0.02
				>980	"	0.15	1.0	8.0	0.73	± 0.08	0.40	± 0.01
				<b>Total</b>		<b>24.13</b>	<b>46.5</b>	<b>2.3</b>	<b>106.0</b>	<b>± 0.77</b>	NA	
				<b>Weighted Avg</b>							<b>0.44</b>	<b>± 0.01</b>

NA-Not Applicable

M- Missing sample

BD- Below Detection

Table 2. Pseudo- $K_d$ s and trap component weight % for OC and ballast minerals for 2005 SV sediment traps

Depth (m)		OC	Lithogenic	CaCO <sub>3</sub>	Opal	bulk $K_d$
313 and 524	$K_d$ (10 <sup>6</sup> g/g)	45.4	4.9	7.3	5.5	7.9
	wt%	3.76	25.0	15.8	21.2	
	% contribution to bulk $K_d$	33	23	22	22	
1918	$K_d$ (10 <sup>6</sup> g/g)	86.3	5.9	6.9	10.4	10.0
	wt%	2.41	27.2	25.3	13.4	
	% contribution to bulk $K_d$	30	24	26	20	

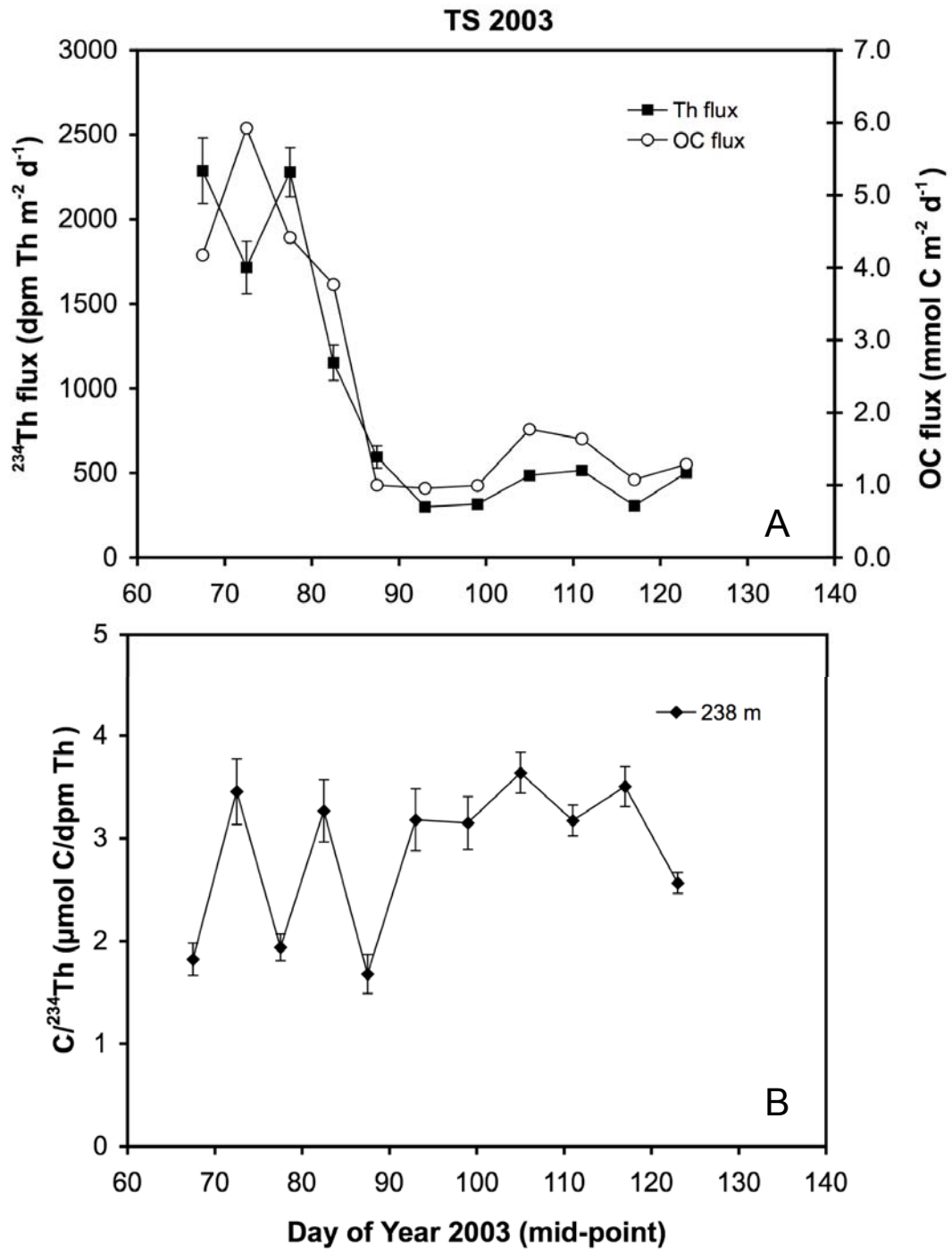


Figure 1

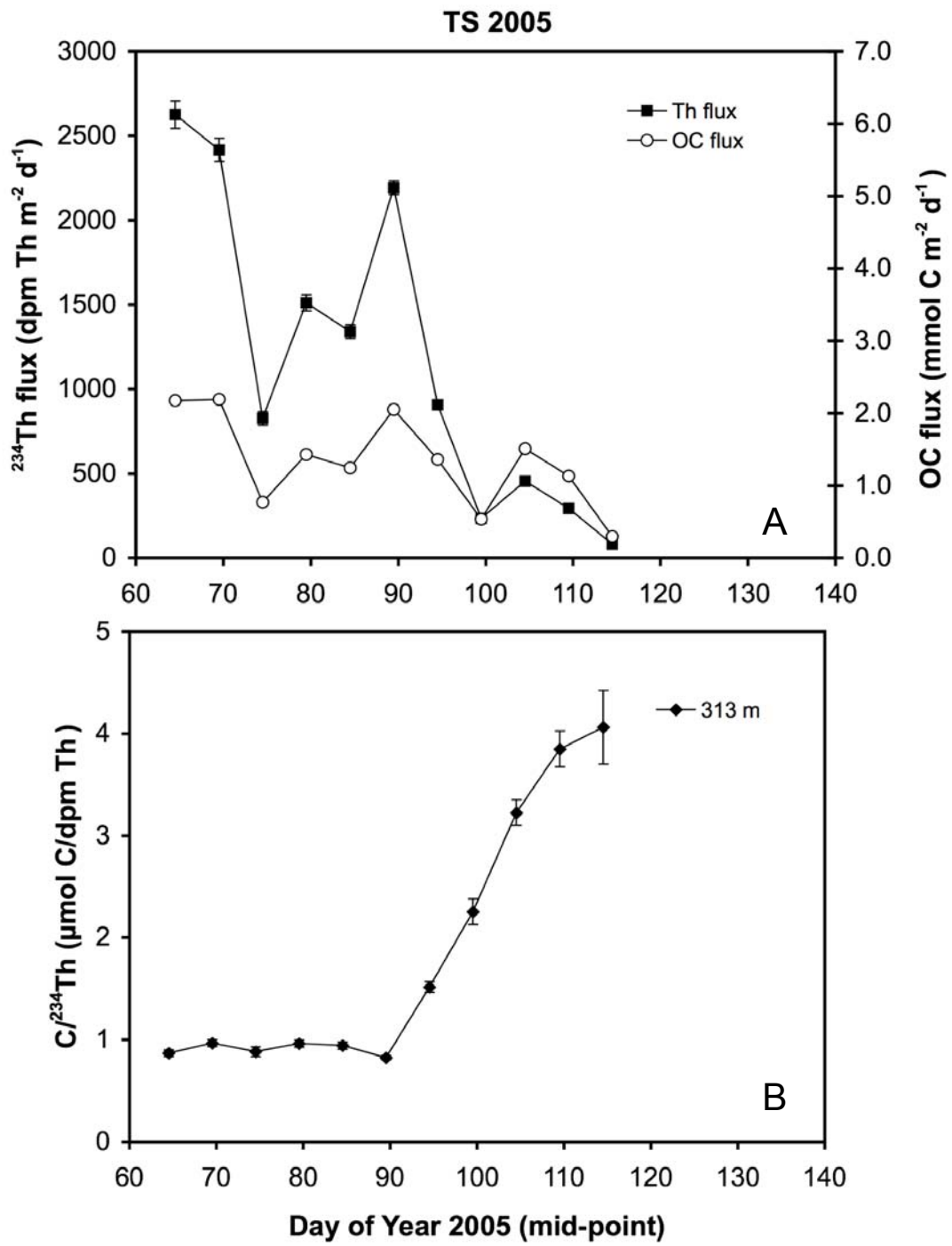


Figure 2

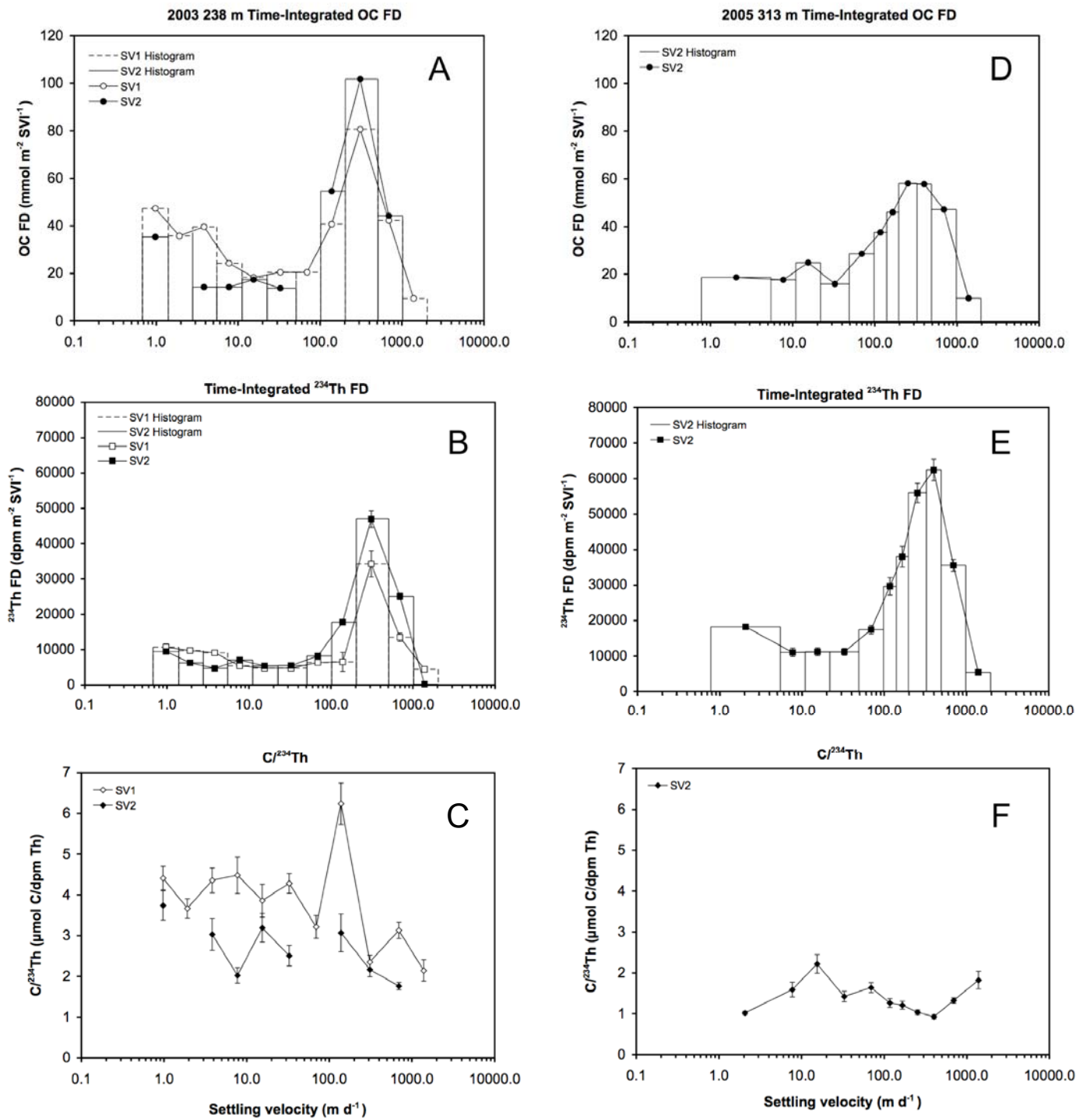


Figure 3

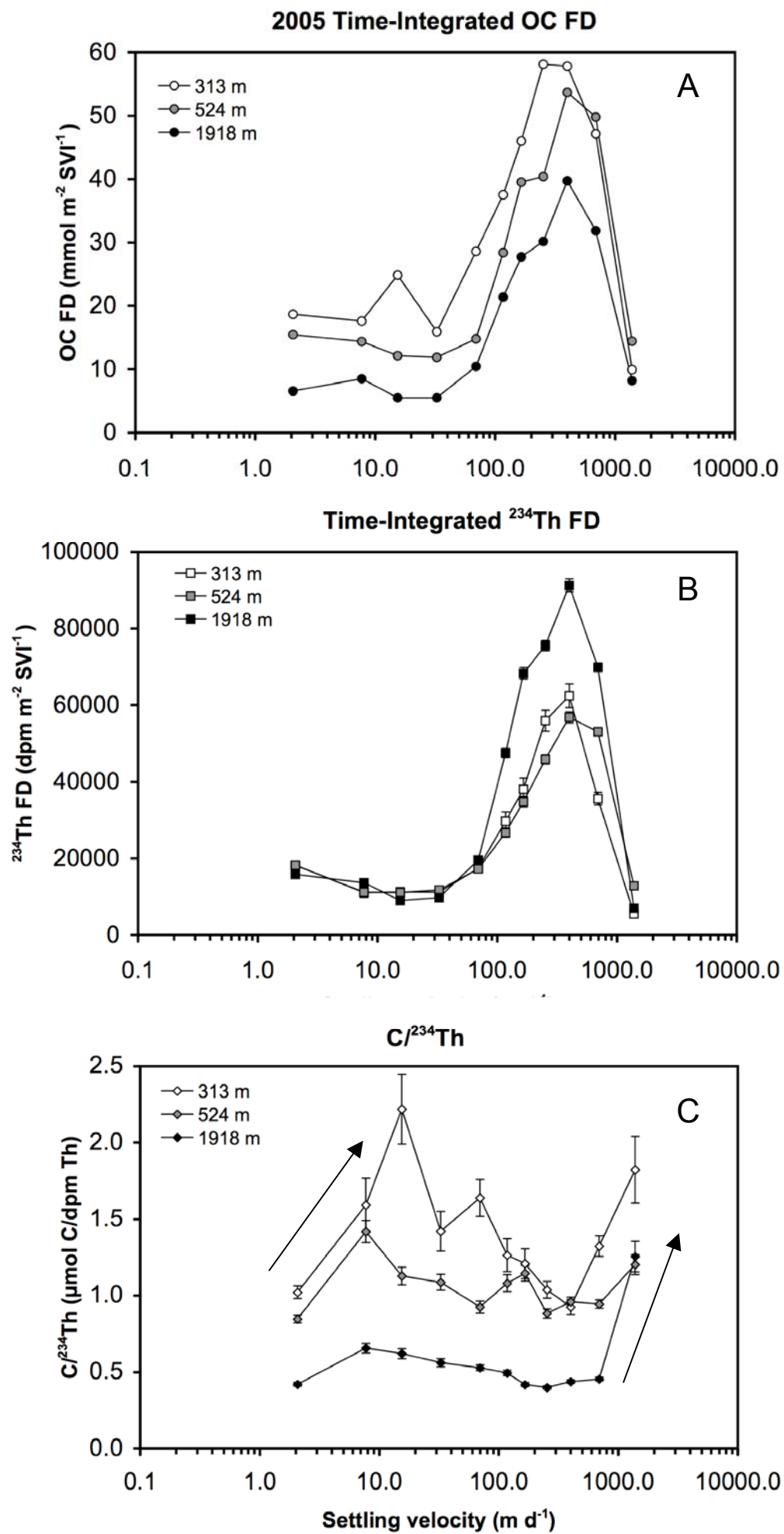
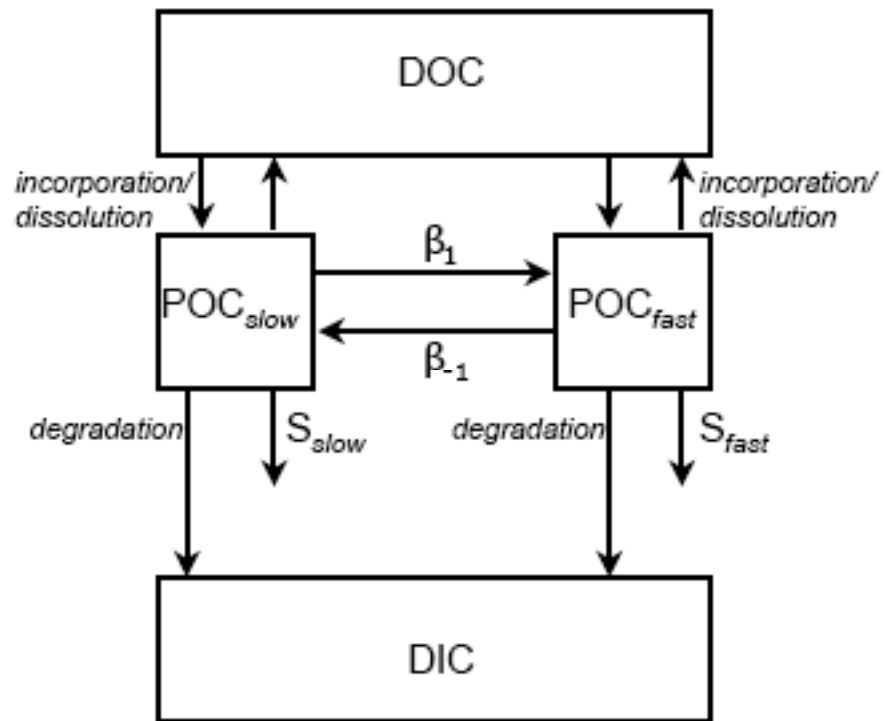


Figure 4

A



B

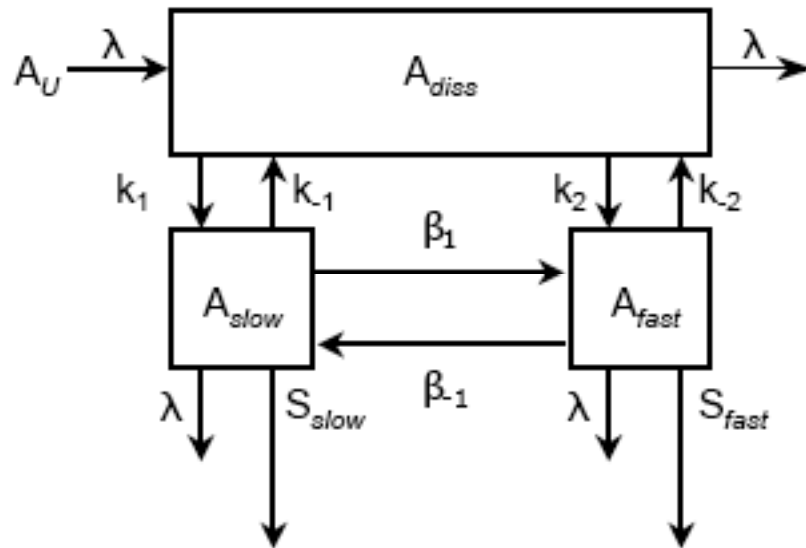


Figure 5

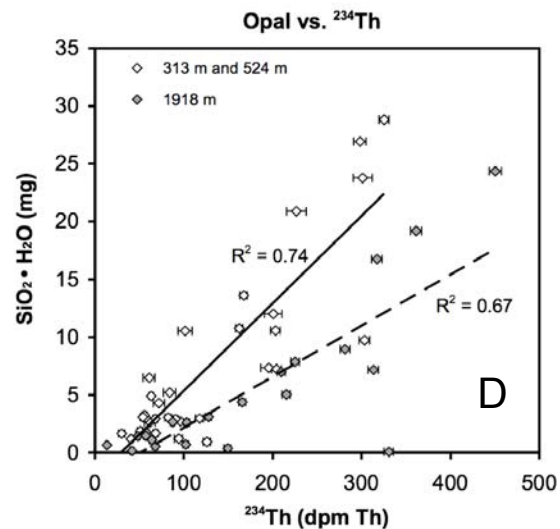
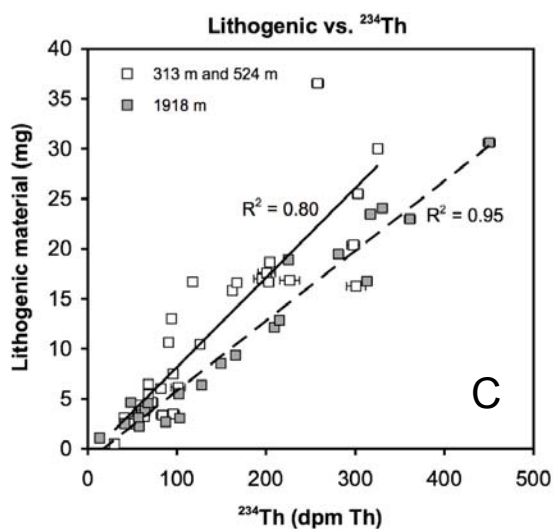
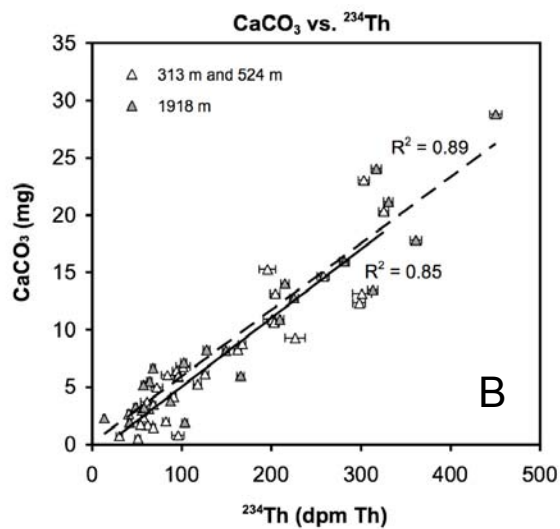
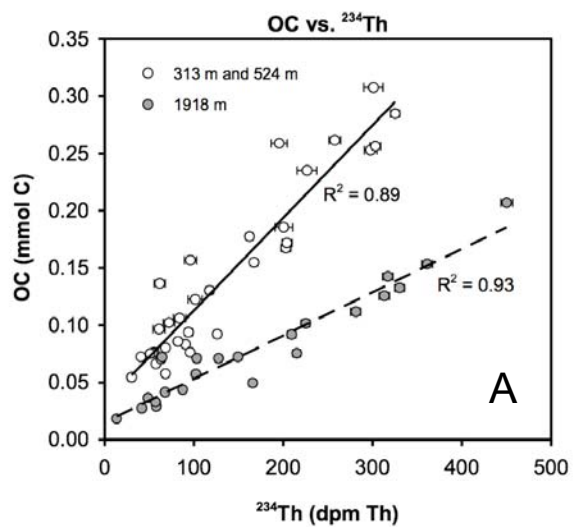


Figure 6